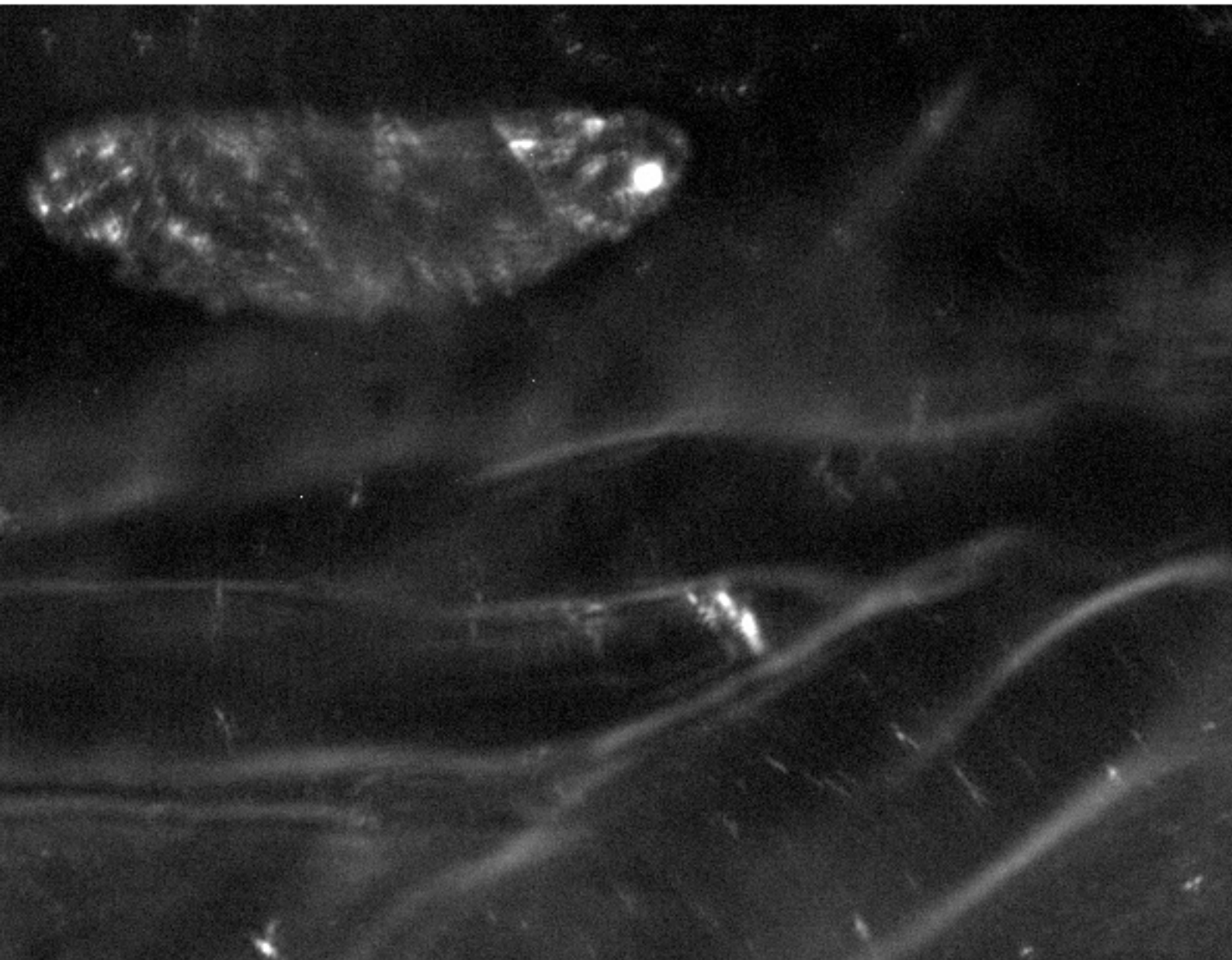


Response of Human Adipose Derived Stem Cells to 5-azacytidine and Zebularine Treatment, Culturing in Methylcellulose-based Medium and Matrix Elasticity



Author:
Morten Petersen

Supervisor:
Vladimir Zachar

Aalborg University 2009

Title:

Response of Human Adipose Derived Stem Cells to 5-azacytidine and Zebularine Treatment, Culturing in Methylcellulose-based Medium and Matrix Elasticity

Theme:

Tissue Engineering

Project period:

P10, The Spring Semester 2009

Project group:

09gr1088b

Attendees:

Morten Petersen

Supervisor:

Vladimir Zachar

Numbers printed: 4

Number of pages: 76

Number of appendices: 4

Finished: 4th of June 2009

Synopsis:

This master thesis focuses on the differentiation of human adipose derived stem cells (ASCs) toward the cardiomyogenic lineage. Based on methods described in the literature, 3 different methods is used. 5-azacytidine (AZA) as well as Zebularine (ZEB) is added to normal growth medium and the response of the ASCs is investigated. Spontaneous differentiation is investigated by culturing the ASCs in a methylcellulose-based medium. Finally, collagen type 1 (COL1) and fibronectin (FIB) crosslinked polyacrylamide (PA) gels is prepared in order to investigate if matrix elasticity influence the differentiation of the ASCs. The results show that neither the AZA and ZEB treatment nor the methylcellulose-based medium can induce differentiation of the ASCs into cardiomyocyte-like cells. It is possible to produce PA gels crosslinked with both COL1 and FIB, however, it is necessary to further develop the fabrication process as the ASCs can not proliferate on these gels.

Preface

The main purpose of this master thesis was to investigate if it is possible to guide the differentiation of ASCs toward the cardiomyogenic lineage. Based on a thorough search and analysis of already published results, three methods were chosen. hASCs were treated with two cytidine analogues, namely AZA and ZEB, which have shown to guide bone marrow derived mesenchymal stem cells (bmMSCs) from both humans and rats toward the cardiomyogenic lineage. Spontaneous differentiation in a methylcellulose-based medium as well as a combination of both chemical inducers and methylcellulose-based medium were also investigated. Finally, COLI and FIB substrates with elasticities resembling the elasticities of nervous-, muscle- and bone tissue were produced and characterized and the response of ASCs to the substrates was examined. Phase contrast microscopy (PCM) was used to follow the change in morphology of the cells when exposed to the different treatments. In order to determine whether or not the ASCs developed toward the cardiomyogenic lineage, the expression of early cardiac markers were quantified by real-time polymerase chain reaction (PCR)

This thesis was conducted by Morten Petersen from Aalborg University, Drug & Tissue Technology, 10th semester. During this project Helle Møller assisted with technical aspects of cell culturing and real-time PCR, Peter Fojan provided information about protein crosslinking and Trine Fink provided information about the theoretical aspects of real-time PCR. I would therefore like to thank these people for their time and effort.

Throughout this project several abbreviations have been used for appendix (App.), equation (Eq.), figure (Fig.), section (Sec.) and table (Tab.). References are shown as numbers enclosed in square brackets and the bibliography can be found at the end of this report.

Morten Petersen

Abbreviations and Glossary

- AA - Acrylic Acid
- AM - Acrylamide
- APS - Ammonium persulphate
- ASCs - Human adipose tissue derived stem cells
- AFM - Atomic force microscopy
- AZA - 5-azacytidine
- bmMSCs - Bone marrow derived mesenchymal stem cells
- BMP - Bone morphogenetic protein
- BSA - Bovine serum albumin
- C - Celsius
- CAD - Coronary artery disease
- CAMs - Cell adhesion molecules
- cDNA - Complementary deoxyribonucleic acid
- CDxx - Cluster of differentiation xx
- COL1 - Collagen type I
- C_t - Treshold cycle
- D - Deflection
- DMEM - Dulbecco's modified Eagle's medium
- DNA - Deoxyribonucleic acid
- ECM - Extracellular matrix
- EDC - N-ethyl-N-(3-dimethylaminopropyl)carbodiimide hydrochloride
- ESC - Embryonic stem cell
- FCS - Fetal calf serum
- FGF - Fibroblast growth factor
- FIB - Fibronectin
- GAGs - Glycosaminoglycans
- HEPES - 4-(2-hydroxyethyl)-1-piperazineethanesulfonic acid
- HUVEC - Human umbilical vein endothelial cell
- MBA - Methylene-bis-acrylamide
- MEF2 - Myocyte enhance factor 2
- MEM - Minimum essential medium
- MES - 2-(N-morpholino)ethanesulfonic acid
- MI - Myocardial infarct
- mRNA - Messenger ribonucleic acid
- MSC - Mesenchymal stem cell
- NHS - N-hydroxysuccinimide
- NTC - No template control
- PA - Polyacrylamide
- PBST - 0.05% Tween20 in S-PBS
- PCM - Phase contrast microscopy
- PCR - Polymerase chain reaction
- PST - Polystyrene
- Px - Passage x
- RT - Room temperature
- S-PBS - Sterilized phosphate buffer solution
- SCs - Stem Cells
- Sulfo-SANPAH - Sulfosuccinimidyl-6-(4'-azido-2'-nitrophenylamine) hexanoate
- T+E - Trypsin + EDTA solution
- TEMED - N,N,N,N-tetramethylethylenediamine
- UV - Ultraviolet
- YM - Young's modulus
- Z - Vertical displacement
- ZEB - Zebularine

Contents

1	Introduction	7
1.1	Stem Cells	8
1.1.1	Mesenchymal- and Adipose Tissue Derived Stem Cells	8
1.2	The Extracellular Matrix	10
1.2.1	Components of the Extracellular Matrix	10
1.2.2	Cell-Cell Interactions	12
1.2.3	Cell-Extracellular Matrix Interactions	13
1.3	Cardiomyogenesis	15
1.3.1	Introduction to Cardiac Development	15
1.3.2	Heart Induction	15
1.3.3	Transcriptional Regulation	16
1.4	Literature Review	17
1.5	Project Objectives	22
2	Methodological Approaches	24
2.1	Protein Crosslinking	24
2.2	Determining Young's Modulus	26
2.3	Real-time Polymerase Chain Reaction	30
3	Materials and Methods	34
3.1	Materials	34
3.2	Methods	34
4	Results	40
4.1	Characterization of Collagen Type I and Fibronectin Substrates	40
4.2	Response of Cells to Collagen Type I and Fibronectin Substrates	43
4.3	Response to Culturing in Methylcellulose-based Medium	47
4.4	Response to 5-azacytidine and Zebularine Treatment	51
5	Discussion	55
5.1	Influence of Matrix Elasticity on Cell Behavior	55
5.2	Matrix Elasticity	57
5.3	Spontaneous Differentiation	58
5.4	5-azacytidine and Zebularine Treatment	60
5.5	Experiment Improvements	61
6	Conclusions	62
7	Perspectives	63

A Chemicals and Equipment	71
A.1 Chemicals	71
A.2 Equipment	72
B Culturing: Areas and Volumes	73
C Primers	74
D Methylcellulose-based Medium	76

Chapter 1

Introduction

The health organization of the United Nations, WHO, stated in the year 2003 that cardiovascular diseases is a world-wide epidemic, which will pose a great threat for the general well being of mankind. Even though the number of cases in the western part of the world is decreasing, the number of cases increases in the rest of the world. It is therefore of great interest to continue the development of new drugs and treatments for cardiovascular diseases.

Cardiac muscle cells need a constant supply of oxygen and nutrients and any partial or complete blockage of the the coronary circulation will affect the cardiac performance. This disease is also known as coronary artery disease (CAD). Coronary ischemia is normally caused by a plaque formation in the wall of the coronary vessel. In severe cases CAD can lead to heart attack or myocardial infarction (MI). MI is basically caused by cardiac cell death due to lack of oxygen. The death of cardiac tissue creates a nonfunctional area and this area is known as an infarct. An infarction can lead to heart stop if it affects the tissue near the coronary artery and if it affects smaller arteries it can cause unpleasant complications.

The treatments used today cannot restore the damaged heart tissue, but it is possible limit the size of the MI and avoid additional complications by preventing irregular contraction and improving the circulation. It is necessary to eliminate the cause of the reduced circulation and this has to be done within a short period of time after the onset of the MI. Even though it is possible to limit the size of the MI, the non-functional cardiac cells will still affect the heart and circulatory system and it would therefore be of great interest to develop a treatment that will restore the damaged tissue.

Regenerative medicine could be the answer to how the damaged cardiac tissue can be restored as regenerative medicine exploits the repair mechanisms of the body. Stem cells (SCs) are the main part of this process as they are capable of differentiating into any somatic cell of the human body. One of the most readily accessible SC sources in the human body are ASCs and it is of great interest to investigate the use of ASCs in relation to various injuries and diseases like MI. This leads to the initiating problem of this study:

Is it possible to guide the differentiation of ASCs toward the cardiomyogenic lineage

1.1 Stem Cells

The definition of a SC is basically a cell that has the ability to self replicate for indefinite periods. Under the right conditions, SCs can develop or differentiate to the different cell types that makes up an organism like the human organism. Humans are in some degree capable of regenerating certain tissues in the body and some animals can even regrow lost parts of the body. It was though an unsolved mystery until the 1950's, where prove for the existence of SCs was established. Experiments on bone marrow proved that some cells in the bone marrow were capable of developing into blood cells.

SCs derived from humans or infants are called adult SCs and they are characterized by being either multi- or unipotent. Adult SCs have so far been isolated from brain-, bone marrow-, peripheral blood-, blood vessels-, skeletal muscle-, skin-, and liver tissue. Before SCs differentiate into a mature cell it goes through one or more intermediate cell types, which is called progenitor or precursor cells. These cells are usually committed to a certain path of differentiation. Another important property of SCs is their ability to develop or transdifferentiate into cell types outside their lineage and germ layer - this property is known as plasticity [1]. Another type of SCs can be derived from the inner cell mass of the blastocyst of an embryo can develop into cells from all the three germ layers, but it was not before 1998 that embryonic stem cells (ESCs) were extracted from human embryos [2].

It is possible to classify SCs based on their potential to differentiate into different cell types. ESCs is said to be pluripotent as they can develop into cell types from the three germ layers. The zygote is actually more potent than ESCs and it is therefore said to be totipotent, because it not only give rise to the embryo but also tissues like the umbilical cord and placenta, which support the growth of the embryo. Another class of SCs is the multipotent SCs, which can differentiate into cells from one or more germ layers but not all cells from the three germ layers. Finally, SCs can be unipotent, which means that they can differentiate along one specific lineage [1, 3, 4].

One of the most extensively studied SCs are the bone marrow derived SCs and this population of SCs can be divided into two subpopulations, namely the hematopoietic stem cells and the bmMSCs. A third subpopulation found in the stroma of bone marrow has been described, however these SCs can develop into the same cell types as bmMSCs and it is therefore believed that they arise from the same population of cells. MSCs are especially interesting in regard to this project, since MSCs can be derived from other tissues in the body and these include cartilage, fat, muscle, tendon and periosteum, where fat is the most abundant source of MSCs [1, 5, 6]. This project will be based on ASCs and a more detailed description of MSCs and ASCs can therefore be found in the following section.

1.1.1 Mesenchymal- and Adipose Tissue Derived Stem Cells

Adult SCs have been considered to be committed to cell lineages specifically cells from the tissues in which the adult SCs reside. However, it has been demonstrated that for instance hematopoietic stem cells can differentiate into hepatic oval cells [5]. The developmental origin of adult SCs are yet unknown, however, it is believed that they are set aside during fetal development. MSCs

are another adult SC source that displays plasticity and can develop into mature cells from both endodermal and ectodermal tissues like bone marrow, adipose tissue, tendon, skin, bone, muscle, brain, liver, lungs, pancreas, among others [5, 7]. Even though the definition of a SC states it can self-replicate for an infinite time period, the MSCs are characterized by a finite lifespan. The number of cell doublings of bmMSCs has been optimized to 38 ± 4 cell doublings before they reach senescence. It should though be noted that it is possible to increase the life-span to 260 doublings by a retroviral transduction of bmMSCs with the telomerase gene [8, 9].

Table 1.1: **Phenotypic profile of human MSCs** *Expression of certain surface markers of both ASCs and human bmMSCs. The table depicts both positive and negative markers and since this table is based on results from different studies some markers have been reported to be both negative and positive. The phenotypic profile of human ASCs and bmMSCs is very similar and this suggests that they have the same developmental origin. Reproduced from [10].*

Surface marker	Human ASC	Human bmMSCs
CD13	+	+
CD29	+	+
CD44	+	+/-
CD49e	+	+
CD54	+	+
CD55	+	+
CD63	+	+
CD73	+	+
CD90	+	+/-
CD105	+	+
CD106	+	+/-
CD144	+	+
CD146	+	+
CD166	+	+
CD3	-	-
CD11b	-	-
CD14	-	N/A
CD19	-	N/A
CD31	+/-	-
CD34	+/-	+/-
CD45	-	-
CD117	-	-
CD62L	-	-
CD95L	-	-

It is believed that MSCs origins from the mesenchyme, which is formed by sclerotomal cells. Both adipose- and bone-marrow tissue origin from the mesenchyme and it is therefore reasonable to believe that ASCs have the same potential as bmMSCs. Zuk et al. [11] described that ASCs in vitro can develop toward the osteogenic, adipogenic, myogenic, and chondrogenic lineages and the immunophenotypic profile presented in Tab(1.1) also suggests that ASCs and bmMSCs have the same developmental origin [10]. Tab(1.1) depicts both positive and negative surface markers or cluster of differentiation (CD) markers. CD markers are a general description of molecular structures, usually proteins, presented on the surface of the cells. Since the expression of markers on the surface differs from cell type to cell type, these markers can be used to make a unique profile of different cell types.

A lot of attention has been focused on the use and potential of ASCs in regard to tissue engineering and methods to guide the differentiation of ASCs toward the adipogenic, chondrogenic, osteogenic and myogenic lineages have already been established [12]. Furthermore efforts are put into investigating the ability of ASCs to differentiate toward the cardiomyogenic, among others.

1.2 The Extracellular Matrix

Even though animals and humans have hundreds of various cell types, these cell types can be classified as being part of tissues, namely blood, epithelial-, connective-, muscular-, and nervous tissue. The different cell types are arranged in certain patterns in order to produce the tissues and organs. The assembly of tissue and organs are determined by molecular interactions at the cellular level. Cells can interact with each other by adhering directly to one another through integral membrane proteins called cell-adhesion molecules (CAMs) or they can interact indirectly through cell-matrix adhesions. This matrix or more specifically the extracellular matrix (ECM) consists of proteins and polysaccharides, which are secreted by the cells. The ECM in animals is involved in various mechanisms like transportation of nutrients, waste and growth factors, cell stability, protection, movement, metabolism, proliferation, communication and differentiation [13].

1.2.1 Components of the Extracellular Matrix

The ECM is composed of three abundant components and these are proteoglycans, collagens and multiadhesive proteins. Proteoglycans are glycoproteins containing polysaccharide chains called glycosaminoglycans (GAGs), which are long unbranched polysaccharides consisting of a repeating disaccharide unit. Proteoglycans is also called the "filler" substance. They form large complexes with other proteoglycans, hyaluronic acid and matrix proteins like the different collagens. The GAGs of proteoglycans are composed of disaccharides with at least one anionic group and the proteoglycans can therefore bind cations like sodium, potassium and calcium. Besides being involved in the movement of molecules within the ECM, proteoglycans have specific functions dependent on their protein core and GAG. An example is perlecan, which is the most secreted protein in basal laminae. Perlecan is involved in crosslinking of ECM components and can also bind certain cell types to the ECM [13].

Multiadhesive matrix proteins are large molecules that are responsible for binding the various types of collagen, other matrix proteins, polysaccharides, cell-surface adhesion receptors and extracellular signaling molecules like hormones and growth factors. The multiadhesive proteins are therefore very important for organizing the components of the ECM. An example is laminin, which is a protein found in the basal laminae. Laminins have, as demonstrated in Fig.(1.1), several binding sites and can bind collagens, lipids, carbohydrates and integrins. Laminins can therefore link cells to the ECM [13].

Another example of a multiadhesive protein is FIB, which binds to integrins and other ECM components such as collagens, fibrin and proteoglycans. FIB consists of two almost identically monomers linked by a pair of disulfide bonds. The monomer can be divided into three modules, type I, II and III, based on

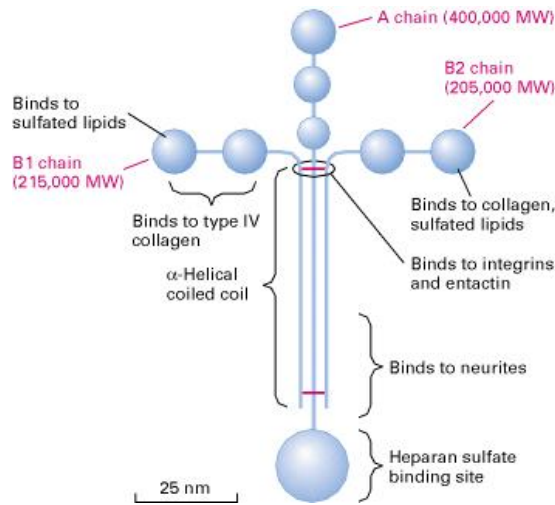


Figure 1.1: **Binding sites on laminin.** Different regions of laminins bind to cell-surface receptors like laminins, carbohydrates, lipids and collagens. From [13].

similarities in the amino acid sequences. The organization of a FIB monomer is depicted in Fig.(1.2) and this figure also shows where FIB binds integrins and other components of the ECM. FIB is important for cell migration and differentiation of many cell types in embryogenesis and fibronectin is also involved in wound healing as it facilitates blood clotting and the migration of macrophages into the wound site [13].

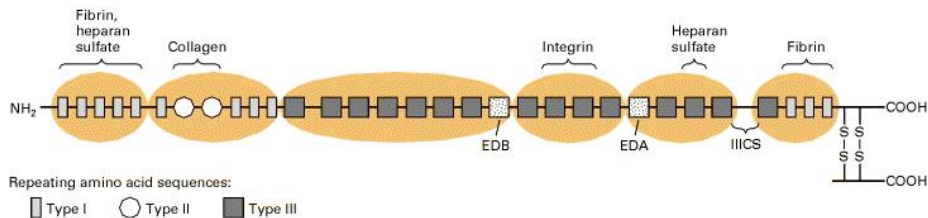


Figure 1.2: **Binding sites on FIB.** FIB is build up by two monomers and this figure only illustrates this monomer. This schematic shows that this monomer has specific bindings sites for molecules like collagens, integrins and heparan sulfate. From [13].

Connective tissue, such as cartilage and tendon, differs from other tissues since connective tissue is mainly made up of ECM. One of the most abundant proteins in the ECM of connective tissue is collagen. Collagens can be divided into several classes based on the type and application and these classes include fibrillar-, anchoring-, transmembrane-, and host-defence collagens. Fibrillar. Collagen type I is very abundant in tendon-rich tissue like rat-tail and due to its easy availability it was the first collagen to be characterized. Collagen type 1 only exists as fibrillar collagens and these fibrils are basically build up by 300 nm long and 1.5 nm thin triple helices composed of two $\alpha 1$ and one $\alpha 2$ chains, which each is composed of 1050 amino acids. The fibrils often aggregate into larger structures known as collagen fibers [13]. The general structure of fibrillar collagens is demonstrated in Fig.(1.3).

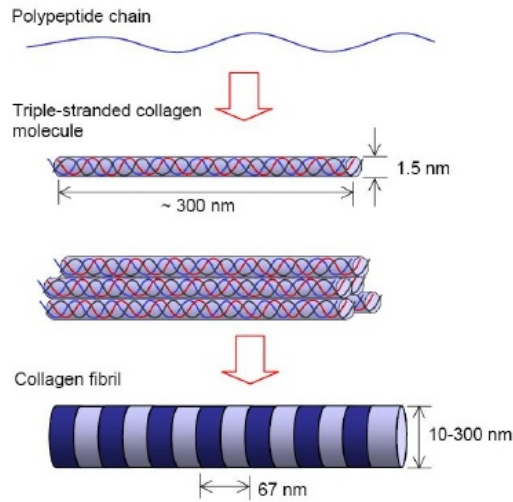


Figure 1.3: **Assembly of fibrillar collagens.** *Collagen fibrils are made up of a triple-stranded collagen helix. This helix is composed of collagen polypeptide chains. From [13].*

1.2.2 Cell-Cell Interactions

Cells attach to each other through CAMs as illustrated in Fig.(1.4) and as the figure illustrates, the interaction between the cells can be divided into two types, namely the homophilic- and heterophilic interactions. Homophilic interactions are found between cells of the same type and heterophilic interactions are found between cells of different types and cells and the ECM. CAMs can be divided into four major families, and these are the cadherins, immunoglobulins, integrins and selectins. CAMs can be distributed across the regions of the plasma membrane that are in contact with other cells or they can be located in small spots or cell junctions. Gap junctions are small and, in most cases, permanent channels between adjacent cells build up by connexin proteins. This junction allow the diffusion of small molecules and ions between the cells. Tight junctions are, on the other hand, used to protect the cells against diffusion and tight junctions are made up of two major types of proteins, namely the claudins and occludins. Another type of junction complexes are the desmosomes, which help to resist shear forces by linking cytoskeletons of cells. Desmosomes are build up by desmoglein and desmocollin, which are members of the cadherin family of CAMs [13].

The cytosol facing domain of CAMs are connected to adapter proteins and these proteins link the CAMs to the cytoskeleton and CAMs therefore influence the cell shape. They also influence the signaling pathways within the cells as the adapter proteins can connect to intracellular molecules, which are involved in pathways that control protein activity and gene expression. Since cell-cell adhesions are associated with the cytoskeleton and signaling pathways, the surroundings of cells influence the shape and the functional properties of the cells. This relationship also works the other way around as the cell, because of its shape and functionality, influence the surroundings [13].

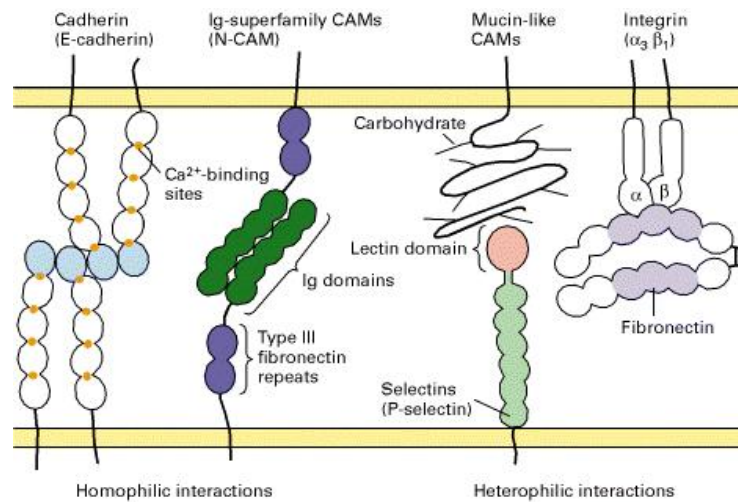


Figure 1.4: **CAMs and adhesion receptors.** Cells can adhere to each other through both homophilic- and heterophilic interactions, where cadherin and immunoglobulin linkages normally are homophilic. Integrins are another class of CAMs and they can also act as adhesion receptors. An example of a heterophilic interaction is the selectin mediated adhesion between adjacent cells. Selectins can bind to glycoproteins and glycolipids. From [13]

1.2.3 Cell-Extracellular Matrix Interactions

Certain cell-surface receptors can bind to components of the ECM and thereby indirectly adhere cells to each other. The interactions between cells and the ECM are heterophilic, as the cell-adhesion receptors like integrins will bind to multiadhesive proteins, collagens and proteoglycans of the ECM. Cells can also interact with the ECM through more specific receptors like the CD surface markers. Like CAMs, the adhesion molecules of the ECM interact with the cells through adapter proteins and the ECM therefore influence the shape and signaling pathways of the cells. This means that a change in the composition of the ECM directly can influence the properties and regulation of the cells [13].

In animals, epithelia and other organized groups of cells are surrounded by a sheetlike meshwork of ECM components known as the basal lamina. In epithelia like the intestinal lining and skin, only one surface of the cells reside on basal lamina, whereas each cell of other tissues, like muscle and fat, is surrounded by basal lamina. The basal lamina is very important for regeneration after tissue damage and it is involved in the embryonic development. The ECM components are mainly produced by the cells that adhere to the basal lamina and the main proteins of this two-dimensional meshwork is collagen type IV, laminins, entactin and perlecan. Cells bind to the basal lamina by the interaction between hemidesmosomes and laminins. The other side of the basal lamina is connected to the underlying connective tissue by collagens fibers. The basal lamina together with the layer of collagen fibers are also called the basement membrane [13].

Non-epithelial cells are not surrounded by basal lamina but are instead connected to the ECM by clusters of adhesive structures called focal adhesions. These protein complexes are not only composed of integrins but also various

other proteins like vinculin. The focal adhesions also interact with the cytoskeleton of the nonepithelial cells and activate adhesion dependent signals for cell growth and motility [13, 14]. In regard to this project, the interaction between non-epithelial cells and the ECM is of particular interest, as it has been shown that the formation of focal adhesion complexes are related to the stiffness of the tissues [15, 16].

When cells adhere to a surface through focal adhesions they pull on the surface through the cytoskeleton in order to sense and react on the resistance. This mechanosensing is mainly performed by the integrins and research suggest that integrin occupancy and clustering regulate downstream signaling in response to the matrix stiffness [14, 17, 18]. Cell mechanosensing is performed over very short distances and if cells are cultured on a feeder layer or coatings on normal culture surfaces, the cells will only react and adapt to the stiffness of for instance the feeder layer. The signals generated through the mechanosensing can results in dramatic changes of the cell phenotype [14, 17, 18].

The matrix stiffness can regulate cell growth, motility, viability and differentiation. Experiments have shown that cells cultured on soft surfaces have a higher cell doubling time as opposed to cells cultured on stiff substrates [14]. Other experiments show that Matrix stiffness can also influence the differentiation of stem cells and precursor cells [19]. Culture plates made of PST are an example of a very stiff surfaces on which fibroblasts and SCs easily can adhere, spread and proliferate, however, these surfaces are very hard compared to the elasticity of the tissues within animals [14].

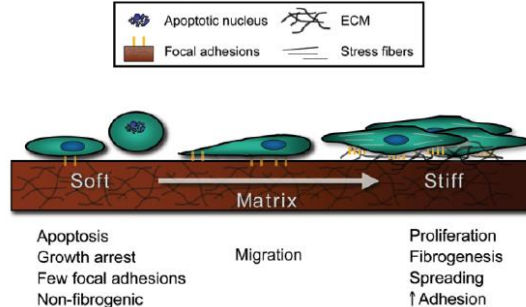


Figure 1.5: **Influence of matrix elasticity on cell behavior.** *Cells cultured on a very soft surface will develop very few focal adhesions and apoptosis can be initiated. As the YM increases, the cells start to migrate and form more adhesion complexes and when the cells are maintained on a stiff surface, the cells spread and develop more adhesion complexes and the stress fibers are formed. From [14]*

Fig.(1.5) illustrates the characteristics of cells cultured on surfaces with an increasing Young's modulus (YM). Cells cultured on a very soft surface will develop very few focal adhesions and apoptosis can be initiated. As the YM increases, the cells start to migrate and form more adhesion complexes and when the cells are maintained on a stiff surface, the cells spread and develop more adhesion complexes and stress fibers are formed.

The stiffness of a surface can be described by YM, which basically is a measure of elasticity. A more thorough explanation of YM and the method used to determine the YM of surfaces can be found in Sec.(2.2). PST culture

plates and flasks have a YM in the GPa range, whereas the elasticity of tissue in animals are in the range of kPa . The YM of tissues in animals varies from hundreds of Pa to MPa . Brain tissue has a YM of hundreds of pa and tendon and cartilage have a YM in the MPa range. Muscle tissue has a YM around 15 kPa [14]. The great difference in elasticity between normal tissue culture plates and the tissues of animals should definitely be considered when describing for instance the differentiation of cells cultured in vitro.

1.3 Cardiomyogenesis

Since this project focuses on guiding ASCs toward the cardiomyogenic lineage, it is of interest to be familiar with cardiomyogenesis during fetal development. The development of the cardiovascular system is a very complicated topic and this section will therefore be an introduction to this field with focus on transcriptional regulation and expression of certain genes, which are of particular interest in regard to this project.

1.3.1 Introduction to Cardiac Development

The development of the vascular system has its onset in the middle of third week, as the embryo no longer can satisfy its nutritional requirements through simple diffusion. Cardiac progenitor cells reside in the epiblast, lateral to the primitive streak. The progenitor cells migrate through the streak and start to develop to cardiac myoblasts. Blood islands also appear and start to form blood cells and vessels. The cardiac myoblasts constitute the myocardium and the blood cells and vessels make up the endocardium. The myocardium and endocardium will fuse and develop into a simple tubular heart. This region is known as the cardiogenic field. The tube will continue to expand but still with an inner endothelial lining and an outer myocardial layer. At some point the myocardial layer will start to secrete ECM rich in hyaluronic acid in order to separate the two layers. During the early existence of the heart, it is composed of these two layers but a third is developed when the heart develops into a loop. This third cellular layer is called the epicardium. The epicardium originates as protrusions from mesothelial cells. The epicardium is the cell source for the development of the coronary arteries. The main three layers are the basis for the development of the heart through the embryonic development [20, 21, 22].

1.3.2 Heart Induction

The myocardial and endocardial cells are provided from three heart fields. These heart fields can be divided into two primary heart fields and a secondary heart field. The primary heart fields are derived from the splanchnic mesoderm and provide the myocardium and endocardium for the primary heart tube. When the heart tube begins to loop, myocardium from the secondary heart field is required. In connection to heart induction, differentiation of myocardial cells and the role of endoderm have been given a lot of attention. The heart fields contain two subpopulations of premyocardial cells and preendocardial cells where the premyocardial cells are more dominant. The specification of myocardial cells is initiated prior to or during gastrulation when the three germ layers are formed.

The induction of the endocardial cell lineage appears to occur at the the same time. The endoderm has a central role in myocyte differentiation as it has been shown that endodermal factors like fibroblast growth factor (FGF) and bone morphogenetic protein (BMP) family members regulates the differentiation of both myocardial and endocardial cells. The FGF family is involved in cardiomyogenesis and studies show that FGF signaling influences cardiomyocyte growth [23]. The myocardium also contain high amounts of FGF-2 in the early stages of heart development and it appears to be important for myocardial cell proliferation. Even though FGF-2 and FGF-4 are the most extensively studied FGFs, experiments on the Zebrafish show that FGF-8 is necessary for the initiation of cardiac gene expression. The Wnt signaling pathways also influence heart induction as inhibition of several Wnt factors induces myocardial differentiation and blood formation. Results show that Wnt antagonist like Frzb-1 and Crescent, which are so called secreted Frizzled-related proteins, can induce the formation of beating cardiac mesoderm when introduced into the lateral mesoderm [21, 22, 24].

1.3.3 Transcriptional Regulation

So far no master regulatory gene that triggers cardiomyogenesis has been identified. In stead the transcriptional regulation of cardiomyogenesis appears to take place via complexes of different transcription factors. The most studied and some of the most important transcription factors are members of the NKX2, GATA and myocyte enhancer factor-2 (MEF2) families [22]. It has been shown that at least five members of NKX2 family are expressed during heart development and the most important member of this family is the NKX2.5 transcription factor NKX2.5 is the earliest marker and the expression of other genes depend on NKX2.5 expression. One of the genes that are dependent on NKX2.5 gene expression is the MEF2C gene. The importance of the NKX2.5 gene has been proven by several studies and Lyons et al. [25] have for instance proved that inhibition of NKX2.5 expression in mice was lethal. Other experiments have also showed that removal of NKX2.5 expression regions results in the loss of corresponding heart structures [26]. Expression of NKX2.5 is regulated by several signaling pathways, where the most important are the Wnt, FGF and BMP pathways. The influence of these pathways has been documented, but the precise molecular mechanisms are to some extend still unknown [21, 22, 27].

Three members of the GATA family are involved in heart development and these are GATA-4, -5, and -6. GATA-4. GATA-5 is only expressed in the endocardium, whereas GATA-4 and 6 are expressed in the myocardium. The expression pattenin of GATA-4 is quite similar to that of NKX2.5 and it is also a an early cardiac marker. GATA transcription factors are involved in the expression of many genes, which encode for contractile proteins like cardiac troponin T and cardiac alpha actin. Furthermore many other genes involved in cardiomyogenesis respond to the expression of GATA transcription factors. Experiments show that mature cardiomyocytes are developed in mice where the expression of GATA-4 has been inhibited as the lack of GATA-4 expression is compensated by other genes [22, 28, 29].

The MEF2 gene family includes four different genes, which are expressed in the precardiac mesoderm and they are also early markers of cardiomyogenesis. MEF2C expression in an embryonic carcinoma cell line up-regulates the

expression of different cardiac genes like GATA-4 and NKX2.5 and other experiments have shown that inactivation of the MEF2C gene leads to termination of cardiac development and furthermore down-regulation of other cardiac genes. Even though a down-regulation is registered, the genes have no specific promoter bindings sites for any MEF2 proteins [22]. This finding suggest that MEF2 proteins act as co-factor and Morin et al. [30] also suggest that MEF2 increases that transcriptional activity of GATA-4.

1.4 Literature Review

The regeneration of cardiac tissue using stem cells is a rapidly expanding field of research. Many approaches have already been published and this review will go through some of the most interesting approaches to guide the differentiation of stem cells toward the cardiomyogenic lineage.

One of the most applied methods in the literature is treating stem cells with AZA. AZA is a cytidine analogue that can be incorporated into both DNA and RNA. When incorporated into DNA, AZA can influence the methylation of genes by covalently binding to DNA methyltransferase. AZA has been used in cancer therapy since it has been shown that DNA methyltransferases are up-regulated in cancer cells. Up-regulation of DNA methyltransferases leads to hypermethylation of genes including tumor-suppressor genes [31, 32, 33]. Methylation of genes is very important for the regulation of gene expression in cells. When inhibiting the methylation of cells, the expression of normally silenced genes can occur and this means that the cell characteristics and even the cell phenotype can change. It has been reported that several hypermethylated genes including the MYOD1 and GATA genes can be reactivated when treating tumors with AZA [31]. Since AZA can reactivate silenced genes several research groups have investigated the effect of AZA treatment on SCs with focus on guiding the SCs toward the cardiomyogenic lineage.

Antonitsis et al. [34] hav investigated the effect of AZA treatment on human bmMSCs. AZA was added to the growth medium to a final concentration of 10 μM . The cells were treated for 24 *h* and then cultured for four weeks. Both real-time PCR and immunocytochemical staining were performed and the staining showed that the cells were positive for beta-myosin heavy chain, whereas the untreated cells only stained positive for vimentin. Real-time PCR analysis was performed on specific cardiac markers including cardiac troponin T and α -cardiac actin and these markers were only expressed in cells exposed to AZA. Xu and co-workers [35] investigated the effect of AZA on human bmMSCs. P2 cells were treated for 24 *h* with AZA and the experiment was terminated after two weeks. Morphological changes were observed after 1 week where the cells had assumed ball- and stick-like structures and after approximately two weeks of culturing myotube-like structures were observed. Both the immunocytochemical staining real-time PCR showed a significant difference in expression of cardiac markers between treated and untreated cells. In order to investigate if the differentiation toward the cardiomyogenic lineage was specific, the cells were also stained with adipo-, osteo- and chondrogenic specific markers and this staining showed the presence of adipocyte-like cells. This indicate that the treatment with AZA is not specific.

Kadivar et al. [36] showed that umbilical cord derived MSCs also can be

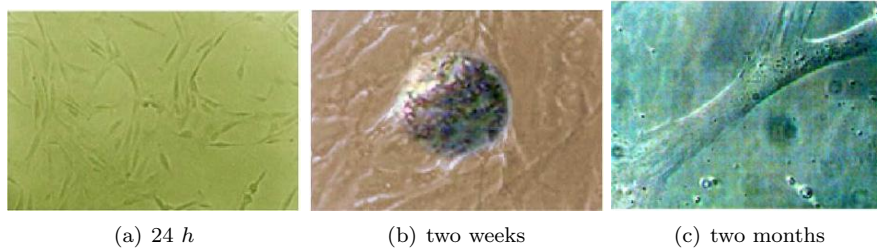


Figure 1.6: **Human MSCs treated with AZA.** (a) The morphology of cells immediately after treatment with AZA. (b) After two weeks some cells have developed into these ball-like structures. (c) The cells developed into myotube-like cells after two months of culturing and the immunocytochemical and real-time PCR analysis also showed that the bmMSCs had developed toward the cardiomyogenic lineage. From [36].

guided toward the cardiomyogenic lineage by treating the cells with AZA for 24 *h*. The concentration of AZA was 6 μM . Morphological changes were observed after two weeks where ball-like structures were observed and after four weeks the cells adjoined and developed into myotube-like cells as illustrated in Fig.(1.6). Real-time PCR proved that the cells had developed toward the cardiomyogenic lineage as an upregulation of specific cardiac genes was observed. Kadivar et al. [36] also proposed that umbilical cord derived MSCs are more suitable for cardiomyogenic differentiation compared to bmMSCs, which in contrary are more suitable for osteogenic differentiation. Several other studies, including Tomati et al. [37], Fukuda et al. [38], Wu et al. [39], Makino et al. [40], and Wakitani et al. [41] have also proved that AZA can induce differentiation of SCs, however, a study published by Liu et al. [42] question the effect of AZA as their results did not indicate that MSCs derived from rats can develop toward the cardiomyogenic lineage. The cells were treated with three different concentration of AZA (3,5 and 10 μM) and two treatments were used, a 24 *h* treatment and a treatment where the cells were treated continuously. Both the immunocytochemical and real-time PCR analysis showed that the MSCs did not express any cardiac markers.

AZA is not the only substance that is capable of inhibiting DNA methyltransferase. ZEB, another cytidine analogue, can also inhibit DNA methyltransferase. Even though AZA and ZEB have almost similar structures, they are very different in relation to stability and half-life. In solution ZEB has a half-life of 504 *h*, whereas AZA only has a half-life of 44 *h*. Studies have furthermore shown that AZA is more unstable and more toxic, however, AZA seems to be more effective than ZEB [43]. A study performed by Lee et al. [44] showed that it was possible to transdifferentiate mouse myoblasts into smooth muscle cells by treating the myoblasts with varying concentrations of ZEB. immunocytochemical analysis showed that the induced cells expressed smooth muscle actin, whereas control myoblasts did not show any expression. Other substances that do not influence the methylation of genes have shown to guide the differentiation of SCs toward the cardiomyogenic lineage. Li and co-workers [45] investigated the effect of Jagged1 protein on MSCs from rats. Jagged1 protein inhibit Notch signaling and the Notch signaling pathway influence cell differentiation. Real-time PCR showed that Notch was highly expressed in the MSCs.

Besides treating the MSCs with the protein, MSCs were also co-cultured with cardiomyocytes for 14 days before harvesting the cells. Their results showed a significant difference in differentiation between MSCs, which were indirectly cocultured with cardiomyocytes and treated with Jagged 1 protein.

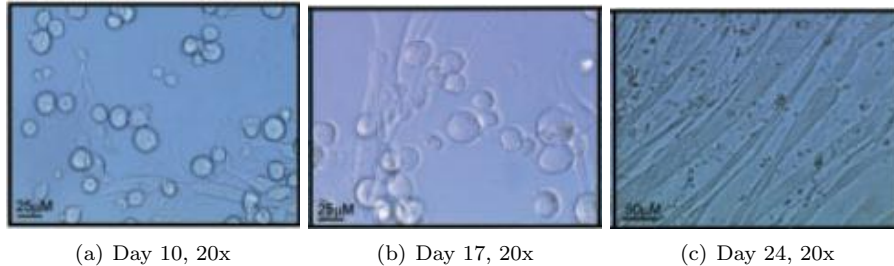


Figure 1.7: **Spontaneous differentiation of ASCs** At day 10 (a) most of cells were rounded but showed contractile activity and at day 17 (b) the cells showed a more elongated morphology. At day 24 (c) the cells had adjoined and myofibrils have been developed. The cells still showed contractile activity. From [46].

The number of studies describing the potential of ASCs in regard to the cardiomyogenic lineage is very limited. A study published by Planat-Benard et al. [46] investigated the development of mouse ASCs when cultured in a methylcellulose-based medium. Methylcellulose increases the viscosity of the medium and the cells are thereby maintained in the medium. Methylcellulose was mixed with Iscove's MDM and supplements. The supplements included insulin, transferrin, mouse stem cell factor, interleukin-3 and 6, among others. As illustrated in Fig.(1.7) the cells were round at day 10 but around day 14 some of these rounded cells showed a contractile activity. The morphology of the cells developed further into cells composed of myofibrils and contractile activity was still observed. Real-time PCR showed that the cells expressed both early cardiac markers, like GATA-4 and MEF2C, and structural genes. Palpant et al. [47] also investigated if murine ASCs could spontaneously differentiate into beating cells when cultured in a methylcellulose-based medium. Contractile cells were observed after 7 days in culture and the Western blotting analysis showed expression of structural proteins. Palpant et al. [47] furthermore showed that the Wnt signaling pathway is involved in cardiomyogenesis as a non-canonical Wnt agonist increased the differentiation potential of the cells a canonical Wnt agonist inhibited cardiac differentiation.

ASCs have been guided toward the cardiomyogenic lineage by co-culturing the cells with extracts from rat cardiomyocytes. Gaustad et al. [48] permeabilized ASCs before suspending them in medium containing cytoplasmic- and nucleatic extracts from cardiomyocytes. After one *h* of coculturing the cells were resealed and maintained in culture for 20 days. The analysis of protein expression showed that 20-25 % of the ASCs expressed cardiac troponin T and desmin and a small proportion of the treated ASCs started to show contractile activity. It was also observed that 40 % of the ASCs developed into multinucleated cells and this also reflects differentiation toward the cardiomyogenic lineage. Another study performed by Haakelien et al. (not published yet) showed that extracts from insulin-producing rat cells can promote insulin synthesis in ASCs. Treating

ASCs extracts from different tissues can definitely be an alternative for inducing differentiation of ASCs, however, the molecular mechanisms underlying the differentiation needs to be addressed. Wang and co-workers [49] did a similar study where bmMSCs from rats were directly and indirectly co-cultured with cardiomyocytes. Indirect coculturing was made by separating the cells by a filter with 3 μm pores. After one week the expression of cardiac markers was examined. BmMSCs that have been in direct contact with cardiomyocytes expressed cardiac markers, whereas the indirect coculturing did not induce differentiation of the cells. These results indicate that soluble factors secreted by cardiomyocytes alone was not enough to guide the bmMSCs toward differentiation and that cell-cell contact was crucial for this process.

A study published by Shim et al. [50] showed that it was possible to produce cardiomyocyte-like cells without the use of cytotoxic substance like AZA or coculturing. They applied a cardiomyogenic induction medium composed of 60 % Dulbecco's modified Eagle's medium (DMEM), 10% fetal calf serum, insulin, transferrin, penicillin, streptomycin, sodium selenite, linoleic acid, ascorbate phosphate and dexamethasone. After the addition of cardiomyocyte induction medium, the MSCs showed expression of both GATA-4 and MEF2C, however, no expression of NKX2.5 was detected. After six passages more than 90 % of the cells stained positive for several cardiac markers including cardiac troponin I and cardiac titin. Even though the cells did not develop into beating cells, Shim et al. [50] suggest that they potentially can be very useful for cell therapy, as the cells have developed toward the cardiomyogenic lineage before engraftment and this could improve the efficiency of cell therapies.

As described in Sec.(1.2.3) matrix elasticity can influence cell behavior and of particular interest, the differentiation of SCs. One of the most used materials to produce surfaces with different elasticities is polyacrylamide gels. The principle behind the production of PA is outlined in Sec.(2.1). PA has several advantages as it is an inert and transparent material, but it is necessary to crosslink proteins to the gel in order to promote cell spreading, proliferation and differentiation. Engler et al. [19] produced PA gels crosslinked with COLI having elastic properties that resembled nerve-, muscle and bone tissue. After seeding of bmMSCs mitomycin C was added in order to inhibit proliferation and then the cells were cultured in normal low glucose DMEM + 20% FCS. The bmMSCs were cultured for 7 days before extracting RNA. 24 hours after seeding a clear difference in cell morphology was observed. BmMSCs cultured on the very soft matrix developed long branches, whereas bmMSCs cultured on the stiff matrix showed an osteoblast-like morphology. The expression of tissue specific markers fit in with the difference in morphology. As illustrated in Fig.(1.8) the immunocytochemical analysis showed that the bmMSCs cultured on the neurogenic matrix expressed $\beta 3$ Tubulin and cells cultured on the myogenic and osteogenic matrix did not express this marker. The same trend was observed on the myogenic and osteogenic matrix, where MyoD and CBF $\alpha 1$ were used as specific markers, respectively. To verify this analysis, a customized oligonucleotide array assay with several specific markers for each tissue was performed. This assay showed an up-regulation of tissue specific markers compared to expression of genes in fresh bmMSCs.

Besides investigating the influence of matrix elasticity on differentiation, Engler et al. [19] also analyzed the expression of focal adhesion complexes and both oligonucleotide assays as well as immunocytochemical analysis showed that the

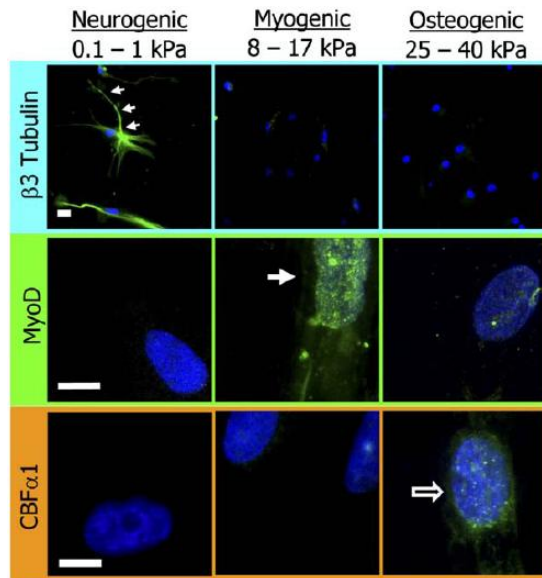


Figure 1.8: **Influence of matrix elasticity on differentiation of bmMSCs.** *The staining of tissue specific markers showed that changes in substrate stiffness influences the differentiation of bmMSCs. $\beta 3$ Tubulin is a specific markers of the neurogenic lineage and it was only expressed in cells cultured on very soft gels. The expression of myogenic lineage marker, MyoD, was only observed on substrates with an elasticity between 8-17 kPa and the expression of CBF $\alpha 1$ was only detected on cells cultured on the stiff substrate. From [19].*

expression of focal adhesion markers increases with substrate stiffness. A similar study was performed by Pelham et al. [15] and their results show that the motility of rat kidney cells decreased with substrate stiffness. The surfaces used in this study were also based on crosslinking COLI to PA gels. Staining of actin and vinculin indicated that focal adhesion complexes were formed when the cells were cultured on a stiff matrix and only very small punctuations of vinculin was observed on the soft matrix. Over time these punctuations of adhesion complexes seemed to appear and disappear, whereas no change was observed in cells on the stiff matrix. This comply with the enhanced motility on soft surfaces. Yeung et al. [16] investigated the response of fibroblast-, neutrophil- and endothelial cells when cultured on both COLI and FIB crosslinked PA gels. Their results suggest that different the three cell types react differently on a variation in substrate stiffness. A change in morphology was observed of endothelial cells, but the proliferation was not affected by the substrate stiffness. When confluency was reached no change in morphology was observed. The formation of stress fibers in fibroblast cells increased with substrate stiffness, however, stress fiber formation was induced in fibroblasts cultured on soft matrices when the cells adjoined. In general the YM of a matrix has to exceed two *kPa* before formation of actin stress fibers was initiated. This stiffness is similar to the elastic modulus of the fibroblasts themselves. Neutrophils on the other hand were unaffected by a variation of matrix elasticity. Circumference measurements showed no increase as opposed to circumference measurements performed on fibroblasts

and endothelial cells. It is not only the substrate stiffness that influence cell spreading. A study performed by Engler et al. [51] showed that both substrate stiffness and COLI concentration have an effect on cell spreading. Smooth muscle cells grown on a soft gel were rounded and cells grown on a stiff gel or glass showed a flattened and polygonal morphology. Variation in COLI concentration had a pronounced effect on cell area when the concentration of collagen was low, however, a plateau was reached at some point before a very high collagen concentration would lead to a decrease in cell area. The formation of focal adhesion complexes and stress fibers were also more distinct on stiff substrates and this result also comply with the cell area measurements. Since both substrate stiffness and COLI influence the formation of adhesion complexes and stress fibers, it could also influence signaling pathways of the cells and thereby proliferation and differentiation.

Another study performed by Engler and co-workers [52] showed that myoblasts can sense and react upon substrate stiffness. Myoblasts were cultured on COLI crosslinked PA gels with varying elasticities. Staining of myosin and actin showed that myotubes developed striations when cultured on substrate with a stiffness similar to the YM of myotubes, whereas almost no formation of striations was observed in cells cultured on very soft- and hard matrices. Differentiation medium was applied after seeding of cells onto the different substrates. The YM of the myotubes used in the study was around 12-15 *kPa*. Another experiment was conducted in order to determine the effect of an underlying cell layer on the formation of striations. The underlying layer was allowed to adhere to the glass surface before seeding the second layer of myotubes. Staining of myosin and actin showed that the top layer of myotubes had developed striations, whereas the bottom layer remained undifferentiated. Deroanne et al. [53] examined how human umbilical vein endothelial cells (HUVEC) would react on variations in substrate stiffness. HUVEC cells cultured on a thin coating of matrigel showed no formation of tube-like structures, instead a monolayer of cells were formed. Gelatin crosslinked PA gels were produced and tube-like structures were only observed on the soft surface. HUVEC cells cultured on the stiff surface developed into a monolayer of cells. This study also show that substrate stiffness can influence the differentiation of cells.

1.5 Project Objectives

The initiating problem states "Is it possible to guide the differentiation of ASCs toward the cardiomyogenic lineage" and with this problem in mind together with the literature review (See Sec.(1.4)), it is possible to make a selection of methods, which will be used to guide the differentiation of ASCs.

One of the most extensively studied methods is the use of AZA. Most studies report that AZA can be used to guide the differentiation of human-, mouse- and rat bmMSCs into cardiomyocyte-like cells. Since ASCs have almost the same phenotypic profile and differentiation potential as human bmMSCs, it is reasonable to test if AZA can trigger differentiation of human ASCs. ZEB is another substance capable of inhibiting DNA methyltransferase and since it is less cytotoxic and has a higher half-life it is a good alternative to AZA. Experiments with AZA have been conducted at the Laboratory for Stem Cell Research at Aalborg University, but the expression of early cardiac markers was

not examined. This leads to first objective of this thesis:

- Examine the expression of MEF2C and GATA-4 of ASCs when induced with AZA and ZEB.

Other methods have been used to differentiate SCs to cardiomyocyte-like cells. Studies performed by Planat-Bernard et al. [46] and Palpant et al. [47] showed that mouse ASCs could develop spontaneously into beating cells. It is therefore of interest to apply the same protocol and investigate if ASCs also develop into cells with cardiac characteristics. The second objective of this thesis is therefore:

- Investigate if ASCs can spontaneously develop into cells with cardiomyocyte-like features.

Matrix elasticity can influence the behavior of both bmMSCs and more mature cells like fibroblasts and endothelial cells. The use of PA gels crosslinked with proteins found in the ECM makes it possible to mimic the elasticities of tissues of the human organism. COL1 and FIB are both found in the ECM of different tissues and both proteins can mediate cell-substrate adhesion. This thesis will focus on preparing PA gels that mimic the elasticities of nervous-, muscle- and bone tissue and then crosslink both COL1 and FIB to the surfaces. This leads to the final objectives of this thesis:

- Prepare COL1- and FIB crosslinked PA gels and characterize these.
- Investigate the response of ASCs when cultured on PA gels that mimic nervous-, muscle- and bone tissue.

Chapter 2

Methodological Approaches

2.1 Protein Crosslinking

As described in Sec.(1.4) it is possible to alter the elasticity of the substrate by varying the amount of methylene-bis-AM (MBA) in the PA solution. PA has various advantages as it is inert and transparent, however, the inactivity is also a disadvantage as the SCs cannot spread and proliferate on the surface. It is therefore necessary to crosslink proteins, which the SCs can recognize and attach to, to the PA gels. This section describes different methods that has been used to crosslink proteins to PA gels.

Principle of Polyacrylamide Gels

Before outlining the crosslinking of proteins to the PA gels, the principle of polymerization of PA gels will be explained. The polymerization reaction of PA gels is identical to that used for gel electrophoresis. In short, the acrylamide (AM) and the crosslinker, MBA, are combined in a solution with N,N,N,N-tetramethylethylenediamine (TEMED) and ammonium persulphate (APS). These two chemicals trigger a polymerization process of the vinyl groups in the AM and MBA monomers as depicted in Fig.(2.1). The double bonds of the vinyl groups will be converted into free radicals and since these free radicals are very reactive, the AA and MBA will react and form PA chains with variable length [54].

It should be noted that oxygen can act as free radical trap and can therefore slow down or even prevent the polymerization process. It is therefore important to minimize the amount of oxygen in the PA solution before adding TEMED and APS and this can be done by either performing the polymerization in vacuum or mixing the substances very carefully.

Sulfo-SANPAH Mediated Crosslinking

One of the most applied methods in the literature is the sulfosuccinimidyl-6-(40-azido-20-nitrophenylamino) hexanoate (sulfo-SANPAH) mediated crosslinking. Sulfo-SANPAH is a photoactivatable heterobifunctional reagent that consists of 2 groups, where 1 group reacts with the PA and the other group reacts with a primary amine. The reaction scheme is illustrated in Fig.(2.2).

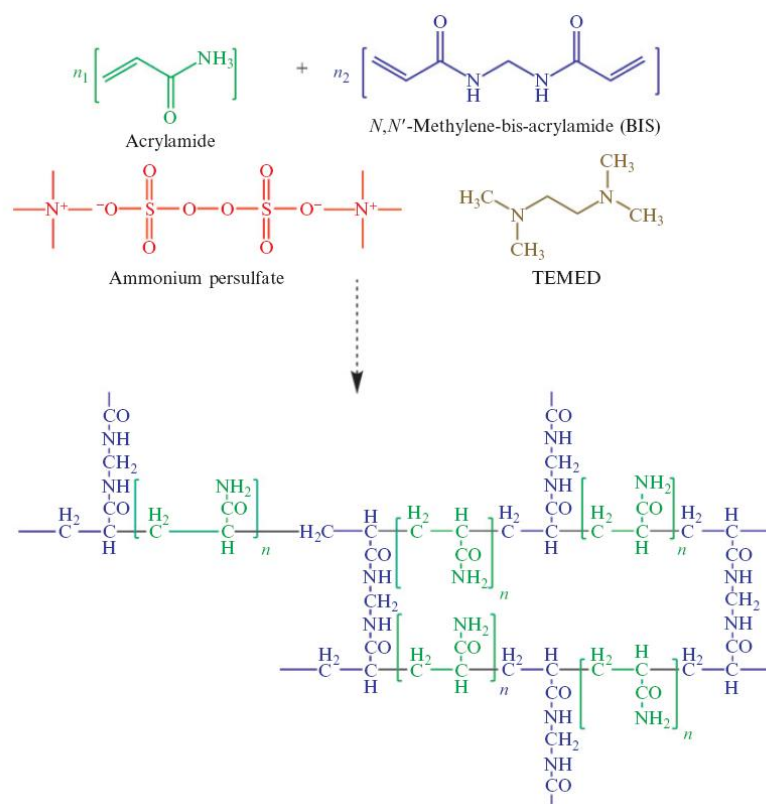


Figure 2.1: **Polymerization of PA gels.** *TEMED* and *APS* trigger the polymerization process of the vinyl groups in the *AM* and *MBA* monomers. The double bond of the vinyl groups will be converted into free radicals, which reacts with *MBA* to form polymers. From [54].

It is necessary to activate the group that reacts with the PA and this is done by exposing sulfo-SANPAH to UV light while the sulfo-SANPAH solution is deposited on the PA gels. When sulfo-SANPAH has been covalently attached to the PA gels, protein is added and the sulfosuccinimidyl group will react with the protein. Even though sulfo-SANPAH has been used extensively, the crosslinker has several limitations, since it has limited solubility, stability and shelf-life [54].

Glutaraldehyde Mediated Crosslinking

Glutaraldehyde is a small molecule with 2 aldehyde groups separated by a chain of 3 methylene bridges. The amino groups of proteins react with the aldehyde groups of glutaraldehyde. When glutaraldehyde is dissolved in an aqueous solution, it is predominantly present as polymers as depicted in Fig.(2.3). Fig.(2.3) also shows that aldehyde groups are available in the polymers. Since PA gels also contain amino groups, glutaraldehyde will react with these and when adding protein to the PA gels after glutaraldehyde treatment the proteins will be crosslinked to the surface. The major drawback with glutaraldehyde crosslinking is the fact that it is very toxic and difficult to wash out of the gel

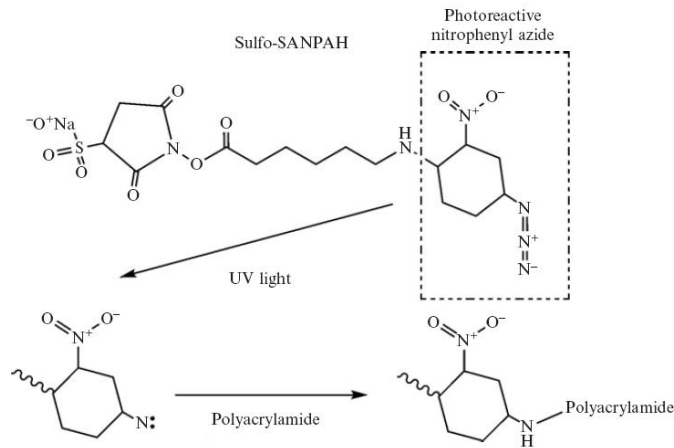


Figure 2.2: **Reaction scheme of the sulfo-SANPAH mediated crosslinking.** *Sulfo-SANPAH is heterobifunctional crosslinker, which means that one group reacts with the PA and the other group reacts with the primary amines of the PA. From [54].*

[55].

Carbodiimide mediated crosslinking

One of the more classical methods used to couple proteins to a substrate, is the carbodiimide mediated crosslinking, which is based on treating the substrate with N-(3-dimethylaminopropyl)-N0-ethylcarbodiimide hydrochloride (EDC). The reaction scheme is illustrated in Fig.(2.4) and this scheme shows that EDC crosslink between free carboxylic acid groups and amines by activating the carboxylic group and thereby creating an unstable ester. An ordinary PA gel does not contain any carboxylic groups but these groups can be introduced into the gel by adding acrylic acid (AA) to the PA solution before initiating the polymerization process. AA is the simplest unsaturated carboxylic acids with a vinyl group at the α -carbon atom and acrylic acid will therefore be a part of the polymerization process by the same free radical reaction as described in Sec.(2.1). Some of the $CO-NH_2$ groups in the PA polymers will be substituted with $-COOH$ groups and the incorporation of $-COOH$ groups into the polymers does not prevent further polymerization, since the MBA will react with the β -carbon atom of acrylic acid. It should be noted that EDC hydrolyzes very easily, however, this can be prevented by adding N-hydroxysuccinimide (NHS) to the EDC solution. Compared to the sulfo-SANPAH mediated crosslinking, this method is more tedious [54].

2.2 Determining Young's Modulus

All objects are deformable meaning that it is possible to change the shape or size of an object by applying an external force. When these changes take place internal forces within the object resist the deformation. This deformation can be described by the terms stress and strain, where stress is the external force

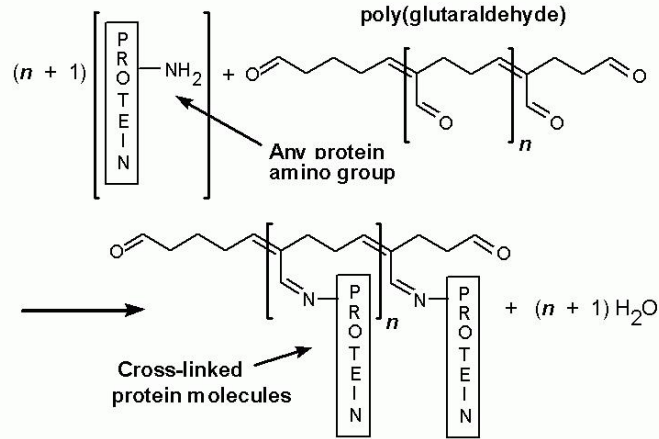


Figure 2.3: **Formation of protein-glutaraldehyde complexes.** *Glutaraldehyde will in solution form polymers and the aldehyde groups of these polymers react with amino groups. Since both PA and proteins have free amino groups, glutaraldehyde can link to both and thereby crosslink them. From [55].*

per unit area acting on the object and the response of the object is the strain. When the stress is small, it has been found that strain is proportional to stress and this constant depends on the material of which the object is composed of. The proportionality constant is called the elastic modulus and this term actually covers three types of deformation, where one of them is the YM. YM is a measure of the resistance of an object to a change in one of its dimensions. Normally YM is used to characterize a rod or wire stressed under tension or compression but YM can also be used to describe other materials like PA gels. It should be noted that the relationship between stress and strain changes if the stress is sufficiently large and the point at which it changes is called the elastic limit. If the stress exceeds this limit the object is permanently distorted and it does not return to its original shape. It is therefore important to apply small stresses when determining YM of objects [56].

When applying stress to an object it will contract or expand in the other two directions. This effect was first described by Simeon Poisson and it is therefore called Poisson's effect. Poisson's ratio is the ratio between the transverse strain, which is perpendicular to the applied stress, and the axial strain, which is in the direction of the applied stress [56]. Most materials have a Poisson's ratio between 0 and 0.5, where it has been determined that PA gels made from a solution containing 10 % AM has a Poisson's ratio of 0.48 [57].

As mentioned earlier the calculation of the YM of the PA gels is based on AFM measurements or more precisely the indentation of the cantilever when approaching the surface. In an AFM the probe is used for local height measurements of the sample surface and the probe is a cantilever, which acts like a spring and therefore obeys Hooke's law. The cantilever can have different shapes depending on the operating mode. At the end of the cantilever is the actual

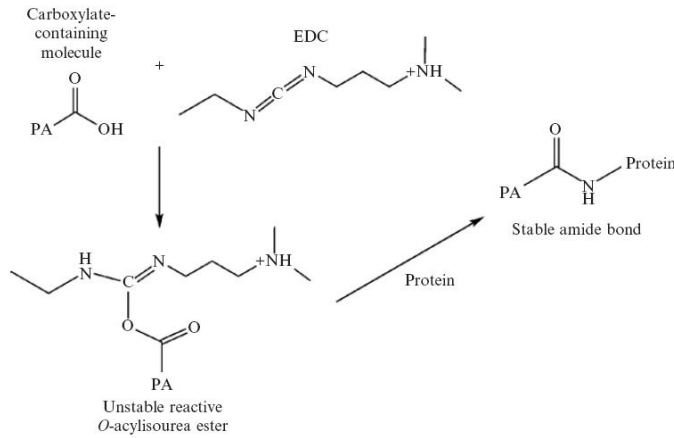


Figure 2.4: **Reaction scheme of the EDC mediated crosslinking.** *EDC can crosslink between carboxylic acids and primary- and secondary amines. The EDC molecule will link to the carboxylic acid group, however, this complex is very unstable and it will react with amino groups if possible. From [54].*

probe or tip, which will interact with the surface. Likewise the cantilever, the tip can have several shapes and the tip applied to perform the force measurements on the PA gels has a conical shape. When the tip moves across the sample surface or approaches the surface during force plots, the cantilever will deflect. As the cantilever bends the reflected light from the laser is displaced and since the spring constant of the cantilever is known, the force of the measurement can be calculated.

An AFM is a very versatile method of measurement as it is possible to use different modes depending on the type of sample and the purpose of the measurement. These two modes are the contact- and tapping mode, where tapping mode normally is applied when scanning soft materials, as contact mode can be rather rough. However, the purpose of these measurements is to compile force-indentation plots and it is therefore necessary to apply contact mode. In order to prevent the tip from staying attached to the PA gels, the measurements are performed in liquid.

The method used to determine the YM of the gels is based on information from Touhami et al. [58] and Vinckier et al. [59]. The mechanical properties of the PA surfaces was investigated by obtaining force calibration plots for each surface. The plots were obtained with the same vertical displacement (Z) and deflection (D). Both Z and D are measured in nm but the deflection can be converted to a force by applying Hooke's law.

$$F = K_c \cdot D \quad (2.1)$$

where F is the applied force, K_c is the spring constant and D is the deflection. An example of a force plot obtained during the AFM measurements is illustrated in Fig.(2.5). Force curves are obtained when the tip is extending and retracting. The curve of interest in regard to the gel elasticity is the force curve obtained during the extension, as this curve describes the deflection of the cantilever when it approaches and enters the PA gel. In order to simplify the calculation

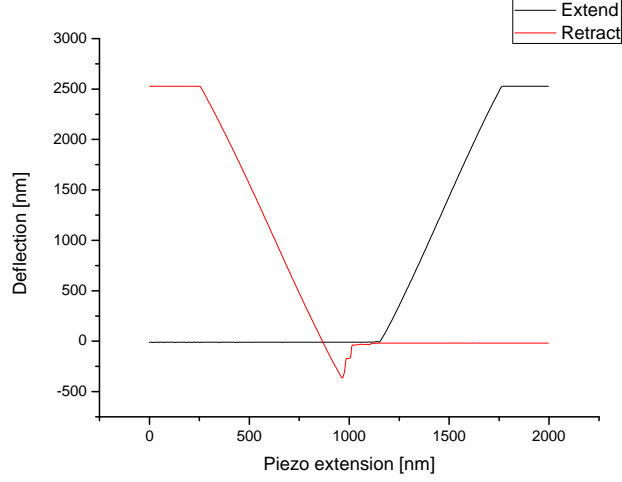


Figure 2.5: **Obtained force plot.** *The extension curve describes the deflection of the cantilever when it approaches the surface and the retraction curve describes the deflection when the cantilever leaves the sample.*

of YM the point where the tip enters the sample is set to (0,0).

The force curves can be used to determine YM by applying simple Hertzian models, which are derived from the continuum of mechanics. These models are valid for elastic surfaces and do not take tip-surface adhesion into account. Since the measurements are performed in liquid the adhesion between tip and surface is minimized and the Hertzian models can therefore be applied. Hertzian models describe the indentation of a non-deformable indenter, which in this case is the AFM tip. It is reasonable to assume that the shape of the silicon nitride tip is maintained during the measurements. The shape of a tip can generally be considered as either conical or paraboloid and the shape of the Veeco NP-20 tip is conical. This means that the model shown in Eq.(2.2) can be applied to determine the elasticity of the PA gels.

$$F = \frac{2}{\pi} \tan \alpha E^* \delta^2 \quad (2.2)$$

where F is the applied force, α is the half-opening angle of the tip, E^* is the surface elastic constant of the material and δ is the indentation. E^* is defined as described in Eq.(2.3).

$$E^* = \frac{E}{1 - \nu^2} \quad (2.3)$$

where E is YM and ν is Poisson's ratio. In order to apply this model it is necessary to compile a force versus indentation plot. The indentation of the tip can be determined by calculating the difference between the deflection of the tip on a hard and soft surface as depicted in Fig.(2.6) and Eq.(2.4).

$$\delta = d_2 - d_1 \quad (2.4)$$

The model describes the relation between applied force and indentation. In order to determine E^* in Eq.(2.2), the applied force versus the indentation is

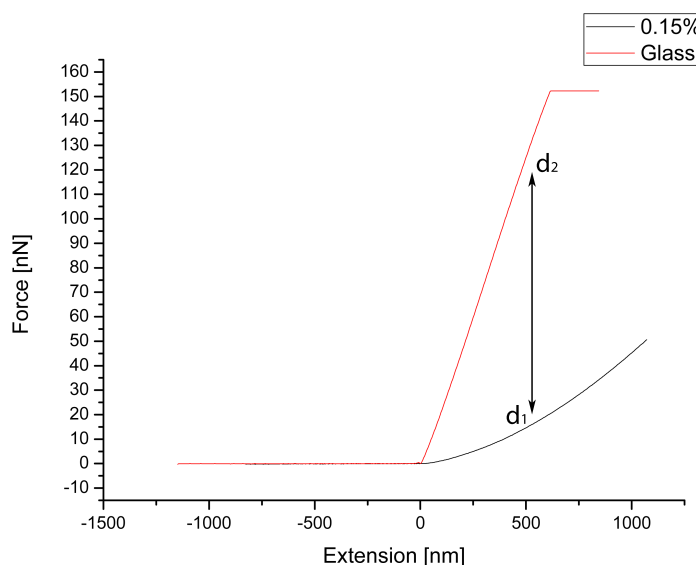


Figure 2.6: **Indentation of cantilever** *The indentation of the cantilever is difference in deflection of the tip on a hard and soft surface.*

plotted and the curve is fitted to a second degree polynomial as according to the model. The applied force versus indentation plot is illustrated in Fig.(2.7). The coefficient to the second degree part of the fit is equal to $\frac{2}{\pi} \tan \alpha E^*$.

According to Boudou et al. [57] the Poisson's ratio of PA gels is 0.47 and by applying Eq.(2.3), it is possible to determine YM of the PA gels.

2.3 Real-time Polymerase Chain Reaction

Real-time PCR is a very useful method if you want to investigate the expression of genes in a cell. This section will give an introduction to the theory behind the method and the method used to quantify the amount of messenger ribonucleic acid (mRNA). Even though real-time PCR is the most preferable method for this purpose, there is still several concerns that have an impact on the reliability of this method and the most common concerns will be described.

PCR is a method that makes it possible to amplify short deoxyribonucleic acid (DNA) sequences of longer double stranded DNA molecule. PCR makes use of a pair of primers, which each is around 20 nucleotides in length and are complementary to one of the two strands of the DNA. After the primers have annealed to the denatured DNA, the primers are extended by a PNA polymerase and a copy of the sequence is made. The DNA is again denatured and primers can again anneal to both the original DNA strands and the synthesized DNA. After primer extension, two copies of the original DNA sequence has been produced. This scenario can continue and after 40 cycles of denaturing, annealing and extension the product can be analyzed on an agarose gel. However, the use of an agarose gel to analyze the results of the PCR amplification is at most semi-quantitative and in order to make the method quantitative, real time PCR was developed. The different reactions set up in a real-time PCR experiment are characterized by a threshold cycle (C_t) value, which is the cycle value where

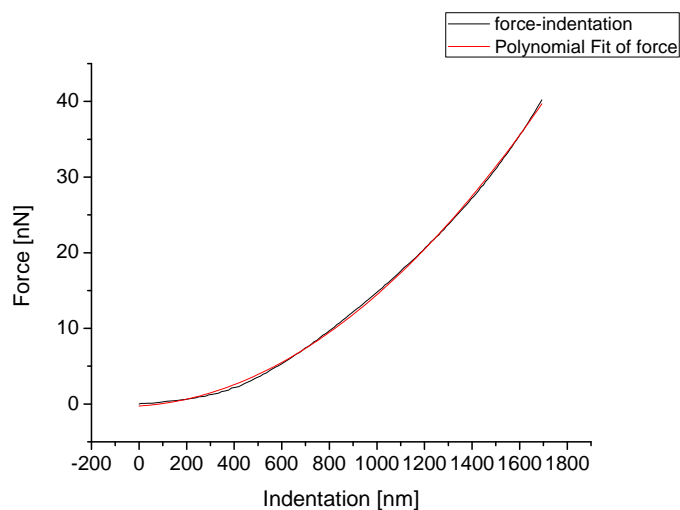
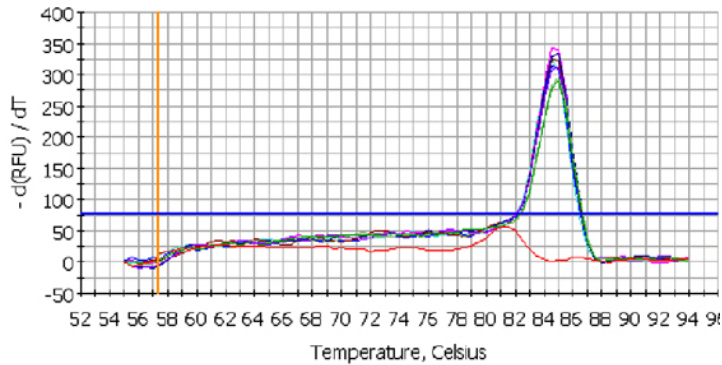


Figure 2.7: **The applied force versus indentation.** *This plot is fitted to a second degree polynomial in order to determine E^* .*

the fluorescent signal rises above a defined or threshold background fluorescence. This means that more starting material will give rise to a lower C_t value. The amplification of a template can be divided into four phases: baseline, exponential, linear and plateau. The baseline phase contains all the amplification below the defined threshold value and even though there is no detectable signal, the template is being exponentially amplified. The exponential phase is comprised by the earliest detectable signal of the amplification and it is during this phase the C_t value is set. The length of this phase depends on the starting concentration of the cDNA and the quality of the assay. In an ideal real-time PCR amplification the efficiency is 100 % meaning that the number of cDNA copies is doubled for every cycle. At some point the efficiency of the amplification will decrease and this is defined as the linear phase. The efficiency will continue to decrease until reaching a plateau. It is not clear why the efficiency of the amplification decreases and reaches a plateau, however, it is very likely that the DNA polymerase will start to denature after going through a high number of cycles [60, 61, 62].

Real-time PCR uses fluorescent reporters to quantify the amount of DNA and this means that the amount of DNA can be measured during the amplification. The applied fluorescent dye in this project is SYBR green, which is a dye that binds to only double stranded DNA and it is also one of the most applied dyes for real-time PCR. The quality of a dye can be described by the ratio of fluorescent signal when the dye is mixed with a solution containing doublestranded- and singlestranded DNA. This ratio is much higher for SYBR green than for instance ethidium bromide. Since SYBR green binds to any double stranded DNA, primer-dimers and non-specific amplification of genes will be detected. It is therefore important to produce a melt curve in order to determine the melting point of the product. The melting point of a doublestranded DNA helix depends on the length of the DNA strand and the base composition. If an amplification has succeeded without any primer-dimer formation or



Melt Peak: Data 10-Mar-03 1259 ed.opd

Figure 2.8: **Example of melt curve** A melt curve is obtained after amplification and as this example shows it is possible to distinguish between correct amplified template and primer-dimers. From [62].

unspecific amplification the melting point of the products will be the same. A typical melt curve produced after DNA amplification is depicted in Fig.(2.8) and this figure shows the difference between the melt curve of primer-dimers and the correct amplified product. A melt curve is produced by increasing the temperature while measuring the fluorescence. As the SYBR green only binds to double-stranded DNA the fluorescent signal will decrease when the doublestranded DNA starts to detach. Before you actually go through with the real-time PCR analysis, it is very important to make sure that the primers can be used. This is done by doing a primer optimization, where the optimal annealing temperature is determined. It is crucial that the designed primers do not form primer-dimers and that the temperature range in which the primers function properly are continuous [60, 61, 62].

The most important part of real-time PCR is to perform a valid data analysis. The applied method in this project is the standard curve method, where a dilution series is used to determine the starting quantity of the samples. An example of a standard curve is illustrated in Fig.(2.9) where the C_t values of the individual dilutions is determined and plotted against the concentration. Based on this standard curve, the starting quantity of the samples can be calculated and it is also possible to determine the efficiency of the reaction as the slope is a measure of this. The formula used to calculate the efficiency is shown in Eq.(2.5). Another very important factor is the coefficient of determination, which describes how well the first degree polynomial fits the curve. The fit needs to be almost perfect if the results should be considered as value. There is not a unambiguous value which this coefficient should surpass, however, the standard curves used in this project should have a R^2 -value of at least 0.98 [61, 63, 64].

$$Efficiency = \left[10^{(-1/slope)} \right] - 1 \quad (2.5)$$

When using the standard curve method, the starting concentration of the samples should be within the dilution series and if this is not the case the ex-

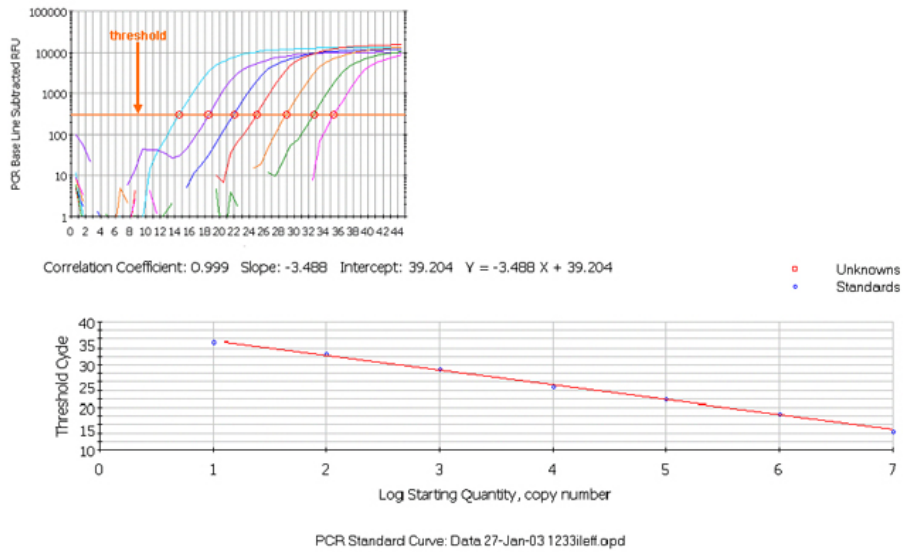


Figure 2.9: **Standard curve example.** Based on a dilution series a standard curve can be composed. This standard curve is used to determine the starting quantities of the other samples. The slope of the standard curve can be used to determine the efficiency of the PCR reaction. From [62].

periment should be redesigned or it is necessary to exclude the data. It is also important to control the C_t values of the samples. The real-time PCR experiments performed during this project are made in duplicates and the difference in C_t value between the duplicates should not exceed $0.5 C_t$. If the difference is higher, it should be considered to redo the experiment. The most important samples in the PCR plates are the no template controls (NTC) and this is because these samples will tell if any contamination has been introduced. The C_t value of the blanks should at least be 5 cycle numbers higher and it is off course preferred that no fluorescent signal is detected from the NTC [61, 63, 64].

There are many pitfalls and concerns, which need to be considered when performing a real-time PCR experiment and it is not possible to account for every concern within this thesis, however, Nolan et al. [64] have described an approach to analyze the results while taking the most general concerns into consideration. This approach will be used when analyzing the results.

Even though the starting concentration of the different samples has been determined based on the standard curve, the starting concentrations cannot be compared before including the expression of control genes or housekeeping genes. It is assumed that the expression of the housekeeping genes is not altered when exposing cells to different environments, however, in most cases it would be preferred to use more than one control gene and then use the geometrical mean as the control gene expression. The ratio of gene expression is determined by calculating the ratio target gene starting concentration and control gene starting concentration. The gene expression is then normalized to the control cells in order to determine if target genes are up- or down-regulated. Since the experiments are performed with duplicates of each sample, the fold increase is imaged as the mean value as well as the standard deviation [60, 61, 62].

Chapter 3

Materials and Methods

3.1 Materials

Materials and equipment details are listed in App.(A). During this project one cell line has been used and this cell line is ASC23. ASC23 cells were harvested from lipowaste taken from the inner thigh of one 42 year old female donor with a BMI of 20.94. The cells were harvested according to protocol described in Zuk et al. [11]. RNA from HUVEC cells, RNA from the SYHY5Y neuroblastoma cell line, total RNA from human skeletal muscle, RNA from ASCs differentiated into chondrocytes, RNA from ASCs differentiated into osteocytes and RNA from ASCs differentiated into adipocytes were used as positive control for cardiac muscle-, endothelial-, nervous-, skeletal muscle-, cartilage-, bone- and adipose tissue, respectively.

3.2 Methods

App.(B) lists the proper amount of S-PBS, medium and trypsin and EDTA (T+E) associated with the different culturing areas. A list of the used primers can be found in App.(C) and App.(D) contains the protocol for preparing the methylcellulose-based medium.

Cell Culturing

The normal growth medium used for all experiments are α minimum essential medium (MEM) + Glutamax with added supplements and these supplements were 10% fetal calf serum (FCS), 1% penicillin and streptomycin and 0.5% gentamicin. Before applying the medium it was poured through a 0.22 μm vacuum filter system.

Thawing of cells: The cells were thawed in tepid water and added to 25 ml normal growth medium. The cell suspension was then spun down by centrifuging at $400 \times g$ for 5 min and RT. The supernatant was decanted and the cells were resuspended in 15 ml fresh medium and added to a 75 cm^2 culture flask. The medium was changed the next day in order to remove unattached and dead cells. The cells were cultured until confluency before using them in experiments.

Resuspension of cells: Medium change was performed every third day if nothing else is stated in the description of the experiments. Medium change was done by removing old medium and then washing the cells with sterilized phosphate buffer solution (S-PBS) before adding fresh medium to the cells.

Splitting of cells: In order to split the cells they have to be detached from the bottom of the PST surfaces and this was done by removing the old medium, washing with S-PBS and adding a proper amount of T+E solution. The cells were then incubated at 37° C for 5-10 *min*. When cells have detached from the bottom, normal growth medium was added in order to inhibit the trypsin. Before seeding the cells, they were manually counted by using a hemocytometer and this was done by first centrifuging the cell suspension at 400 $\times g$ for 5 *min* and RT, decanting the supernatant and resuspending the cells in a low volume of medium. 10 μl of this cell suspension was added to 10 μl Trypan blue and the solution was mixed before transferring 10 μl of the solution to the hemocytometer.

Chemical treatment of ASCs P1 cells were seeded at a density of 1500 cells/cm² in 6-well culture plates and cultured in normal growth medium for 24 hours before adding the induction medium. The induction medium was prepared by adding AZA and ZEB to the normal growth medium and it was prepared immediately before use since the activity of AZA and ZEB decreases over time. Medium was changed every third day and all experiments were terminated after 13 days.

Spontaneous differentiation Two different protocols were used to induce spontaneous differentiation. The methylcellulose-based medium was prepared as described in App.(D). P1 cells were mixed with the medium to a final concentration of 7000 cells/cm³ and the solution was then transferred to four wells in a 12-well plate. At day 13 and 26 cells from a well were lysed and stored for further use. Since some cells adhered to the bottom of the PST culture plates and other cells were maintained in solution, two lysis samples were made for each well. The same medium and cell concentration were used for the second protocol but both P1 and P8 cells were used as well as the cells were induced with AZA and ZEB. After 24 *h* of cell culturing AZA and ZEB were added to the medium. The ASCs were lysed after 13 days of culturing.

Cell culturing on COLI and FIB crosslinked PA gels P1 ASCs were seeded at a density of 1000 cells/cm². Normal growth medium was applied and it was changed every third day. At day 13 the cells were lysed.

Preparation of PA Gels

The glass was rinsed by heating the glass with a bunsen burner, then treating the glass with a 0.1 *M* NaOH solution and finally ethanol. After the glass has dried it was immersed in a 0.4 % bind-silane solution. The glass was washed extensively in demineralized water and air dried. PA gels were prepared by adding AM and methylenebisAM to demineralized water. In order to polymerize the PA solutions 10 % APS (1/200) and TEMED (1/2000) were added to the

PA solutions. The solutions were then deposited onto the bind-silane treated glass and left for polymerization for 30 *min*. The gels were made uniform by using 0.2 *mm* spacers and repel-silane treated glass. Repel-silane treated glass was prepared by immersing the rinsed glass in a repel-silane solution for 10 *min*. The treated glass was then rinsed with demineralized water.

Sulfo-SANPAH Mediated Crosslinking

When the gels had polymerized they were rinsed with a 200 *mM*, *pH* 8.5 HEPES buffer and then blot dried. Approximately 50 μ l 50 *mM* sulfo-SANPAH in 200 *mM* 4-(2-hydroxyethyl)-1-piperazineethanesulfonic acid (HEPES) buffer was added to each surface and the gels were then exposed to 5 *min* of ultraviolet (UV) light with a wavelength between 340-385 *nm* in order to activate the crosslinker. The sulfo-SANPAH solution was then removed from the surfaces and the photoactivation step was repeated. The PA gels were then rinsed with the HEPES buffer and a 0.2 *mg/ml* COLI solution was added to the surfaces. The COLI surfaces were then set for incubation over night at 4° C. Finally the gels were washed extensively with HEPES buffer.

Glutaraldehyde Mediated Crosslinking

After polymerization of the PA gels, a 15% glutaraldehyde in 200 *mM* phosphate solution was added to the gels, which then were set for incubation for 15 *h* at RT. The surfaces were then washed extensively with a 25 *mM* phosphate buffer before adding COLI (0.02 *mg/ml*) and FIB (0.02 *mg/ml*). The gels were then incubated over night at 4° C and washed extensively with S-PBS to remove any unbound glutaraldehyde.

EDC/NHS Mediated Crosslinking

0.4% AA to the 5/10% AM and 0.*xx*% MBA solution. It was necessary to increase the amount of APS (1/25) and TEMED (1/250) if the gels were to polymerize within 15 minutes. After polymerization MES buffer was added to the gels and then set for stabilization for 24 *h*. After stabilization a solution containing 26 *mg/ml* EDC and 0.6 *mg/ml* NHS was added to the gels and set for incubation for 2 *h* at RT. The gels were then rinsed extensively with MES buffer before adding COLI (1 *mg/ml*) and FIB (0.1 *mg/ml*). The gels were then set for incubation over night at 4° C and then rinsed extensively with S-PBS before seeding the ASCs.

Immunostaining of Collagen Type I and Fibronectin Substrates

The COLI and FIB substrates was washed two times in S-PBS before adding the primary antibody. Anti-COLI or anti-FIB was added in a 1/1000 ratio and dissolved in a 1% bovine serum albumin (BSA) in S-PBS solution. The surfaces with primary antibody were then set for incubation for 1 *h* at room temperature. The primary antibodies were removed and the surfaces were washed 3 \times 3 *min* with S-PBS. Anti mouse Alexa Fluor 555 was dissolved in a 1% BSA in S-PBS solution and added in a 1/200 ratio. After the addition of the secondary

antibody the surfaces was set for incubation for 35 *min* at room temperature. The COLI- and FIB substrates were washed 3×3 *min* with S-PBS and left in S-PBS. The Dsred filter cube was applied.

Adsorption of Proteins to Polystyrene

FIB was diluted in S-PBS and a minimal volume of FIB solution was added to the PST surfaces yielding a concentration of $5 \mu\text{g}/\text{cm}^2$. The PST surfaces was then allowed to air dry at RT for 45 *min* after which excess FIB was aspirated. COLI was diluted to a working concentration of 0.01 % using miliQ water. The PST surfaces was then coated with $5 \mu\text{g}/\text{cm}^2$ and set for incubation at 37° C for several hours. Excess COLI solution was removed and the surfaces were air dried before rinsing with S-PBS.

Elasticity Measurements

The elasticity of the PA surfaces was measured with an AFM and the measurements were performed in liquid and contact-mode in order to prevent adherence of the cantilevers to the PA gels. The Veeco NP-20 cantilever has a silicon nitride tip and a spring constant of $0.06\text{N}/\text{m}$. The samples were placed on the piezo element and the AFM head was then mounted. The distance between sample and cantilever was manually decreased before adding approximately 0.2-0.3 *ml* miliq water to the cell. The cantilever was approached to the surface through the software and force calibration plots were obtained when the tip had reached the surface. Force calibrations plots were obtained at a speed of $0.5 \mu\text{m}/\text{s}$ and the deflection range as well as the ramp size were set to $2.0 \mu\text{m}$.

Enzyme-linked Immunosorbent Assay

In order to block unspecific binding sites on the PA gels crosslinked with COLI and FIB a 1% BSA in S-PBS blocking solution was added to the surfaces and incubated for 1 *h* at 37° C. The PA gels were washed with S-PBS before adding primary antibodies, which were primary antibody mouse monoclonal anti-fibronectin and anti collagen type 1. The primary antibodies were diluted in 1% BSA in S-PBS (1/1000). After incubation for 1 *h* at 37° C, the surfaces were washed 4 times with a 0.05% Tween20 in S-PBS solution (PBST). Anti-mouse immunoglobulin conjugated with horseradish peroxidase was diluted in 1% BSA (1/1000) and a suitable amount was added to the PA gels. The gels were then set for incubation for 1 *h* at 37° C. The secondary antibodies were removed and the gels were washed 4 times with PBST. 1,2-phenylenediamine was dissolved in deionized water containing 0.0125% hydrogen peroxide and a proper amount was added to each surface. The surfaces were then set for incubation at 37° C until a satisfactory yellow color was obtained. 0.5 *M* sulfuric acid stop solution was then added to the gels and 100 μl product was transferred to a 96-well microtiter plate before reading the absorbance at 490 *nm* using the Victor plate reader.

Extraction of Ribonucleic Acid

Adherent ASCs were lysed by adding 350 μ l lysis buffer containing 1% mercaptoethanol to each well and the lysis sample was then mixed with 350 μ l 70% ethanol and transferred to the column. ASCs cultured in the methylcellulose-based medium were lysed by first adding Ischove's MDM to the wells in order to reduce the viscosity of the solution. The solution was then mixed thoroughly and centrifuged at 14000 $\times g$ for 5 *min* and RT. The supernatant was decanted and 350 μ l lysis buffer containing 1% mercaptoethanol was added to the ASCs. After mixing 350 μ l 70% ethanol was added to the lysis sample and the solution was then transferred to a column. The column was centrifuged at 400 $\times g$ and 20° C for 1 *min*. The supernatant was decanted and 700 μ l low stringency wash was added to the column and centrifuged at 14000 $\times g$ for 1 *min* and RT. The supernatant was decanted and 10 μ l DNase 1 in 70 μ l DNase digest buffer was added to the column and set for incubation for 15 *min* at RT. The column was then centrifuged at 14000 $\times g$ for 1 *min* and RT and the supernatant was decanted. 700 μ l high stringency wash was added to the column and the column was centrifuged at 14000 $\times g$ for 1 *min* and RT. The supernatant was decanted and 700 μ l low stringency wash was added to the column and centrifuged at 14000 $\times g$ for 1 *min* and RT. The supernatant was decanted and the column was centrifuged for additional 2 *min*. The supernatant was decanted and the column was transferred to a new tube containing 0.5 μ l ribonuclease inhibitor. 80 μ l Elution buffer heated to 70° C was added to the column and set for incubation at RT for 1 *min*. The column was centrifuged 14000 $\times g$ for 2 *min* and RT and the column was removed.

Production of Complementary Deoxyribonucleic Acid

Before the cDNA was produced the concentration of the RNA was determined. The samples was normalized to the sample with the lowest concentration in order to obtain the same amount of cDNA. The total reaction volume was 20 μ l and the amount of Iscript reverse transcriptase and Iscript reaction buffer 5 \times was 1 μ l and 4 μ l, respectively. Only RNA was added to the reaction mix of the sample with the lowest concentration and otherwise the concentration was adjusted with nuclease free water. The reaction protocol for the PCR reaction was 5 *min* at 25° C, 30 *min* at 42° C, 5 *min* at 85° C and finally 5 *min* at 4° C.

Real-time Polymerase Chain Reaction

Before preparing the plates, the samples were diluted to the maximum concentration the amount of cDNA allows for. Before use, the primers were diluted to a concentration of 10 μ M. A master mix was produced and this master mix contained SYBR green supermix, water and the diluted reverse- and forward primers. The master mix was transferred to the PCR tubes and the diluted cDNA was then mixed with the master mix before transferring it to the PCR plate. All samples were prepared in duplicates. The primer optimization performed on every primer showed that the real-time PCR can be performed at 62° C. The reaction protocol for the real-time PCR was 3 *min* at 95° C followed by 40 cycles (15 *sec* at 95° C, 30 *sec* at 62° C). After finishing the template

amplification, a melt curve was obtained. The primers used are depicted in App.(C).

Statistics

Students t-test was used to determine if there was any significant difference in crosslinking of proteins to the 3 different PA gels applied in this project. Students t-test was chosen because it was assumed that the population was normally distributed, however, the sample size was so small that the statistic is not normally distributed.

Chapter 4

Results

4.1 Characterization of Collagen Type I and Fibronectin Substrates

In order to verify that the COLI is crosslinked to PA surfaces the surfaces were stained based on the protocol described in Sec.(3.2). ASCs were used as a positive control and a PA gel without any crosslinked protein as a negative control. The positive control proved that the antibodies were functional and the negative controls proved that there was no unspecific binding of the antibodies.

Images obtained after staining of COLI and FIB crosslinked PA gels are illustrated in Fig.(4.1).The images show that all three methods can be used to crosslink COLI and FIB to the PA gels. Even though the protein layers are not uniform, the EDC/NHS mediated crosslinking seems to be the most reliable method. Even though the protein layers are not uniform, the amount of protein could be enough for the cells to adhere, spread and proliferate.

The reason for the varying crosslinking of COLI and FIB when applying sulfo-SANPAH could be the low stability of sulfo-SANPAH when it is dissolved. The efficiency of the glutaraldehyde crosslinking also varies and the protein layers are not uniform. The reason for this could be that glutaraldehyde polymers react with the amino groups in the gel the crosslinking of protein is thereby prevented.

Since the use of COLI substrates is based on information from Engler et al. [19], the concentration of MBA in the polyAM gels is between 0.03 % to 0.6 %, where the highest concentration should yield the lowest elasticity and thereby the highest YM. YM is determined based on the method described in Sec.(2.2)). The force plots obtained from the AFM measurements are illustrated in Fig.(4.2) and these plots show that the indentation of the cantilever increases when the concentration of MBA decreases.

Based on the force plots, the YM of the surfaces was calculated and the results are shown in Tab.(4.1). It should be noted that all elasticity measurements are performed without any protein crosslinked to the surface as results published by Engler et al. [51] showed that COLI crosslinked to PA gels does not influence the elasticity.

It was expected that the calculations of YM would yield the same result, namely that the YM increases when the concentration of MBA increases. This

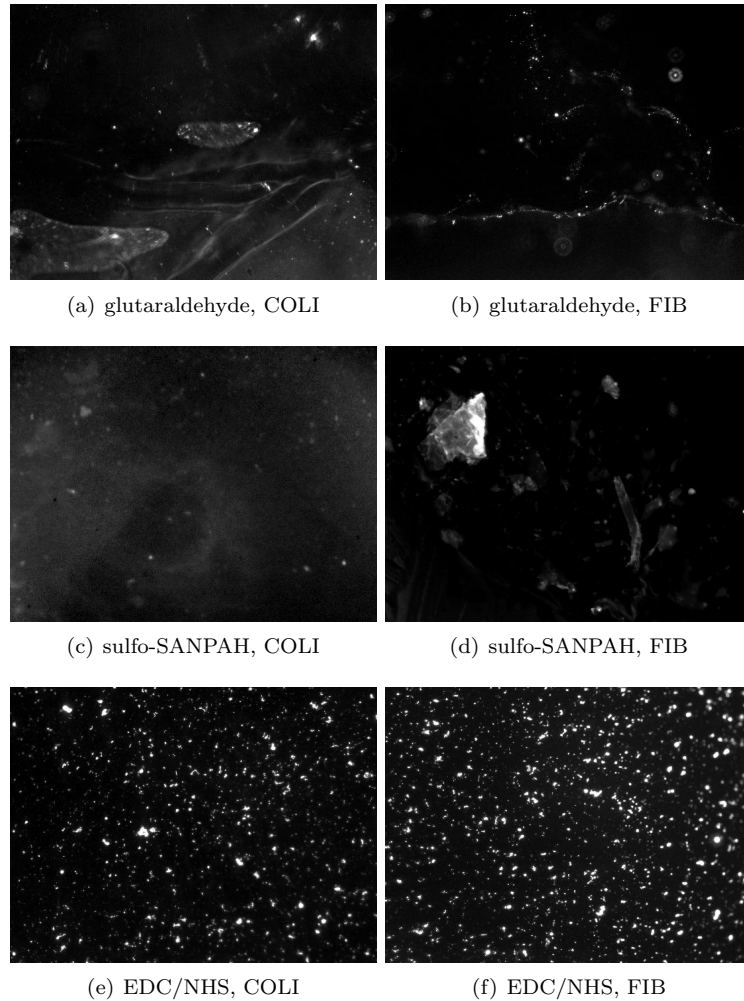


Figure 4.1: **Staining of COLI and FIB.** *These images indicate that both COLI and FIB can be crosslinked to PA gels by using the three different crosslinkers. However, the protein layers seem to be more uniform on PA gels, where EDC/NHS has been used to crosslink COLI and FIB.*

Table 4.1: **Young's modulus measured in Pa of PA gels** This table shows the calculated YM of the PA gels as a function of the concentration of MBA. The YM of both PA gels with and without AA has been determined and furthermore the results from Boudou et al. [57] are shown in the table. It should be noted that the results from Boudou et al. are read off a graph.

Conc. of AM	Conc. of MBA in %	PA gels	PA gels with AA	[57]
10 %	0.03%	2523	6238	5000
10 %	0.15%	4640	13713	30000
10 %	0.30%	22332	45300	40000
5 %	0.03%	N/A	555	1000

also corresponds to the results published by Boudou et al. [57]. The YM of PA gels containing AA was higher compared to PA gels without AA. Since the

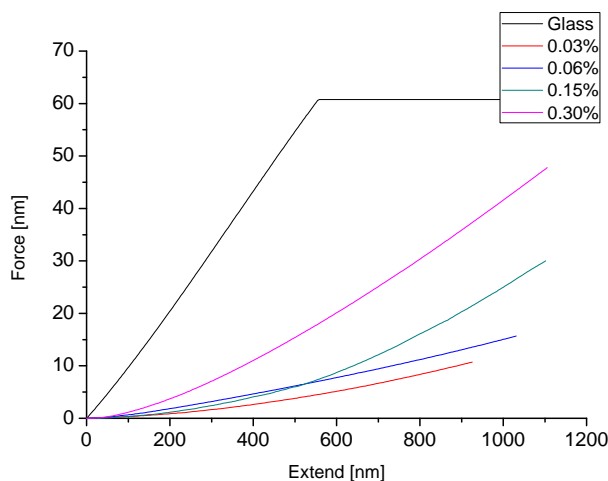


Figure 4.2: **Force plots based on AFM measurements.** *The PA gels were made from a solution containing 10 % AM, 0.4 % AA and a concentration of MBA ranging from 0.03 % to 0.60%*

mechanism behind the polymerization of AA is the same as AM, the addition of 0.4% AA could influence the length and complexity of the PA meshwork.

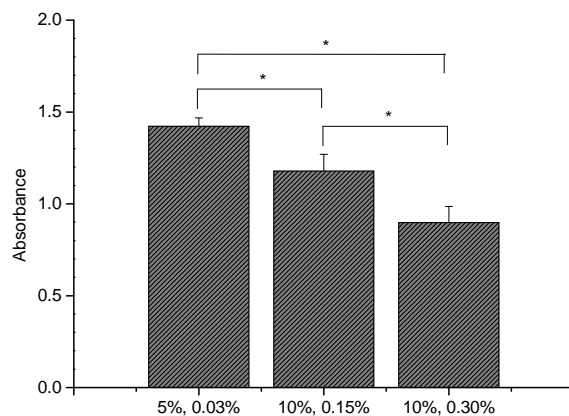


Figure 4.3: **Relative amount of COLI crosslinked to PA gels.** *ELISA was performed in order to investigate if the stiffness of the PA gels influence the amount of COLI crosslinked to the PA gels. Student's T-test proved that there was a significant difference between the 3 different PA gels and the amount of crosslinked COLI decreases as the stiffness increases. * $P < 0.05$.*

It proved impossible to form gels that resembled the elasticity of nervous tissue when using a concentration of 10% AM. The elasticity of gels can also be altered by de- or increasing the AM concentration and a solution containing 5% AM and 0.03% MBA proved to have a YM around 500 Pa. In the light of the

YM calculations and the YM of nervous-, muscle and bone tissue it was decided to use three different gels for further experiments. These are the 5% AM and 0.03% MBA, 10% AM and 0.15% MBA and 10% AM and 0.30% MBA gels.

The amount of MBA and AM was varied in order to control the elasticity of the PA gels and it could be of interest to investigate if this variation influences the amount of COLI crosslinked to the PA gels. This was investigated by using ELISA and the applied protocol is described in Sec.(3). Student's T-test was used to determine if there was any significant difference between the amount of COLI crosslinked to the PA gels. The statistical analysis proved that there is a significant difference in the amount of COLI crosslinked to the 3 PA gels and that the amount of crosslinked protein decreases as the stiffness of the PA gels increases.

4.2 Response of Cells to Collagen Type I and Fibronectin Substrates

The staining proved that the EDC/NHS mediated crosslinking was the most efficient, however, it is necessary to culture cells on the surfaces in order to determine if the cells can adhere, spread and proliferate. ASCs were seeded on the surface with a density of 3000 *cells/cm*² and PCM images were obtained after three days of culture. The images are depicted in Fig.(4.4).

The images clearly show that the ASCs can only adhere and spread on the surfaces, where the EDC/NHS mediated crosslinking was applied. The staining showed that COLI and FIB in some degree was crosslinked when applying glutaraldehyde and sulfo-SANPHAH but the cells could not survive on these surfaces. This indicate that the amount of crosslinked protein on the surfaces is not sufficient for the ASCs to adhere and spread. Glutaraldehyde is very toxic and during the crosslinking procedure the PA gels were treated with glutaraldehyde for at least 15 hours before adding COLI or FIB. Before seeding any cells on the glutaraldehyde treated surfaces, the surfaces have to be washed extensively in order to remove the glutaraldehyde. When medium was added to the surfaces, it changed color from red to yellow and this clearly indicates that there was glutaraldehyde left in the wells. Since ASCs only spread on PA gels where COLI and FIB have been crosslinked by applying the EDC/NHS method, this method was used to produce COLI and FIB crosslinked PA gels with varying elasticities.

An experiment was setup in order to investigate the response of ASCs to culturing on PA gels with elasticities corresponding to nervous- muscle- and bone tissue. 2-well glass slides were used and P1 cells were seeded at a density of 1000 *cells/cm*². The response of the ASCs toward matrix elasticity was investigated by PCM. After two weeks of cell culturing the experiment was terminated and the cells were lyzed for further analysis by real-time PCR. ASCs cultured on a normal PST tissue culture plate were used as a control and they spread and proliferated as expected. PCM images of ASCs cultured on COLI crosslinked PA gels are shown in Fig.(4.5). At day 2 the ASCs had spread on the surfaces and the morphology of ASCs cultured on the 5%, 0.03% gel was more round, whereas a elongated morphology was observed on the other two gels. At day 6 it was expected that the ASCs would have proliferated, however, the cell doubling

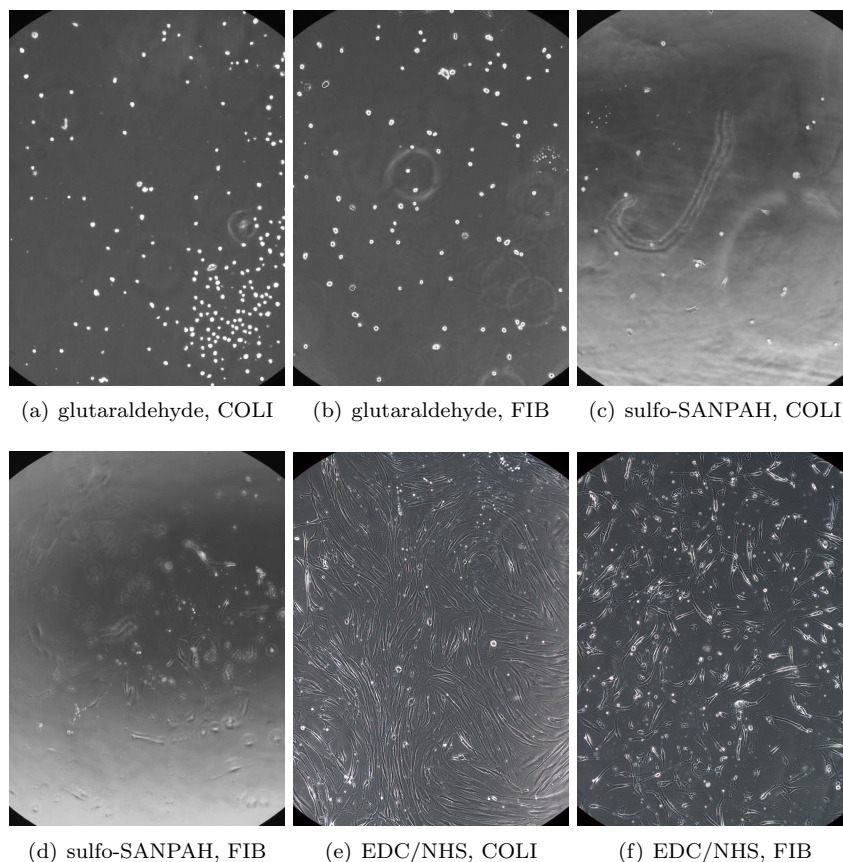


Figure 4.4: **Response of ASCs to COLI and FIB crosslinked PA gels.** *These PCM images show that cells were able to spread on COLI and FIB crosslinked PA gels, EDC/NHS was applied as the crosslinker.*

times were higher for these ASCs compared to the cells cultured on a normal tissue culture plate. The morphology seemed to be independent of the matrix elasticity after 6 days of culturing. At day 14 the cell density on the three gels remained the same as seen at day 6. ASCs on the 10%, 0.30% gel were larger compared to day 6. One explanation to the low cell density seen after 14 days is that many of the seeded cells stay round throughout the 14 days of culturing. They did not spread nor proliferate.

ASCs were also cultured on FIB crosslinked PA gels and PCM images obtained after day 2, 6 and 14 are illustrated in Fig.(4.6). At day 2 some of the ASCs had spread on two of the surfaces, whereas ASCs cultured on the softest (5%, 0.03%) gel had maintained their round morphology. The morphology of ASCs cultured on the 10%, 0.15% and 10%, 0.30% gels was very similar. At day 6 the ASCs on the soft gel did not spread and there was no change in cell density from day 2 to day 6 of ASCs cultured on the two other surfaces. However, ASCs cultured on the 10%, 0.15% gel had spread more. ASCs on the 10%, 0.30% gel showed no difference in cell morphology from day 2 to day 6. No change in cell density was expected at day 14, however, an increased cell density was observed on the 10%, 0.30% gel. The cell density observed on this gel did not represent

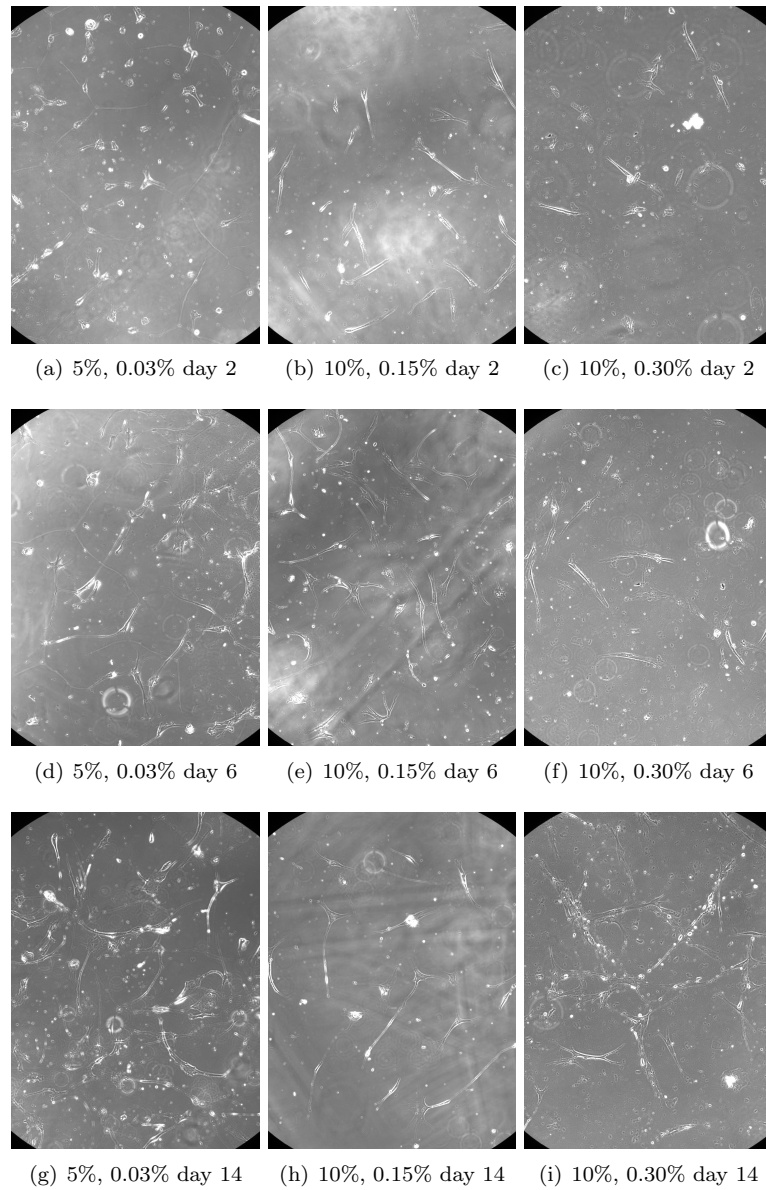


Figure 4.5: **Response of ASCs to COLI crosslinked PA gels.** *At day 2 the morphology of ASCs cultured on 5%, 0.03% gel was more round compared to the other two surfaces. At the at day 6 the cells had assumed a more elongated morphology. ASCs cultured on the 10%, 0.15% and 10%, 0.30% gels showed an elongated morphology throughout the period of culturing. Based on the morphology, the matrix elasticity did not have an impact on the differentiation of the ASCs. It was furthermore expected that the cell density would increase throughout the period of culturing, however, this was not the case.*

the entire gel. This could be explained by a poor cell seeding leading to a higher concentration of cells in the center of the well. The ASCs were round on the

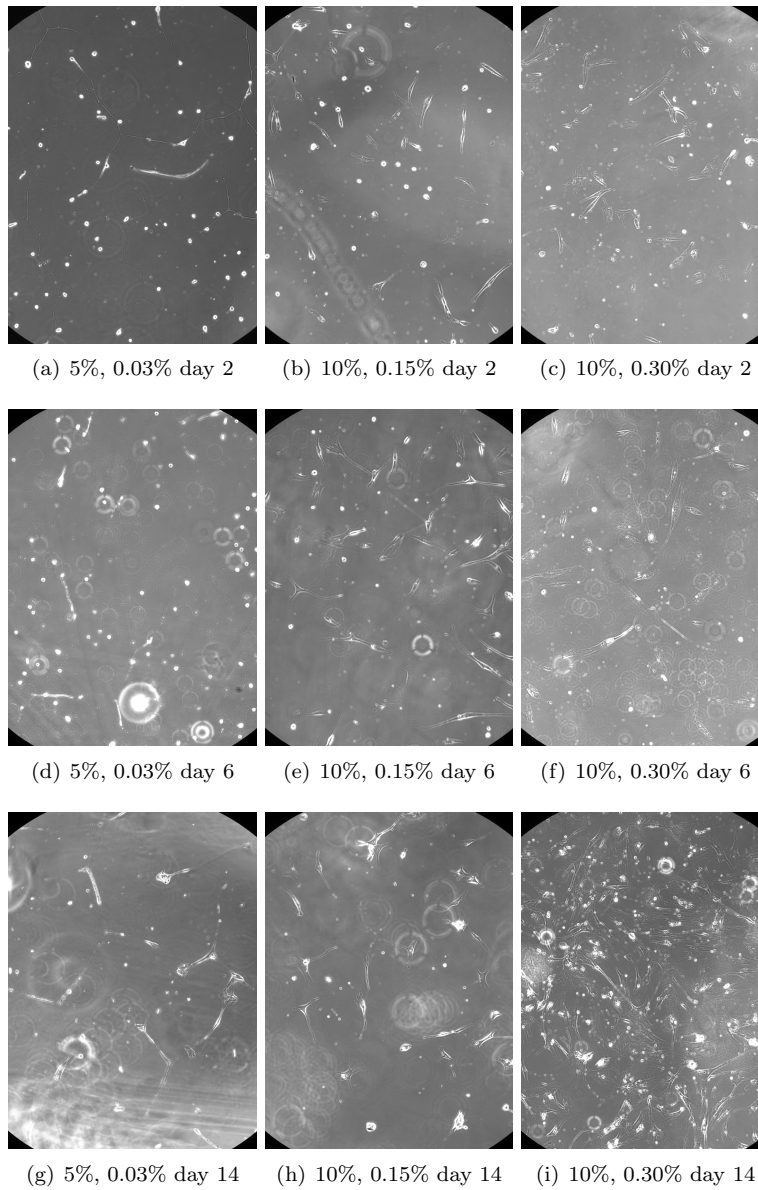


Figure 4.6: **Response of ASCs to FIB crosslinked PA gels.** *The same trends were observed on the FIB crosslinked PA gels as the ASCs cultured on the 5%, 0.03% showed a round morphology, whereas ASCs cultured on the other two surfaces spread. From day 2 to day 6 there was no difference in cell density and the ASC on the 5%, 0.03% gel stay round. At day 14 the cell density had increased of the ASCs cultured on the 10%, 0.30% gel. This increase in cell density was not observed on the entire gel.*

5%, 0.03% gel and no change in morphology was neither observed on the 10%, 0.15% gel.

4.3 Response to Culturing in Methylcellulose-based Medium

Spontaneous differentiation of ASCs was performed by adding P1 ASCs to a methylcellulose-based medium indented for hematopoietic SCs. Two different protocols were applied as described in Sec.(3.2). The first protocol did not involve any addition of AZA and ZEB. As illustrated in Fig.(4.7), the ASCs both adhered to the bottom of the PST culture plates and they were maintained in the medium. After 13 and 26 days, lysis of the ASCs was performed. Two lysis samples were produced in order to allow for individual real-time PCR analysis of adherent and non-adherent cells.

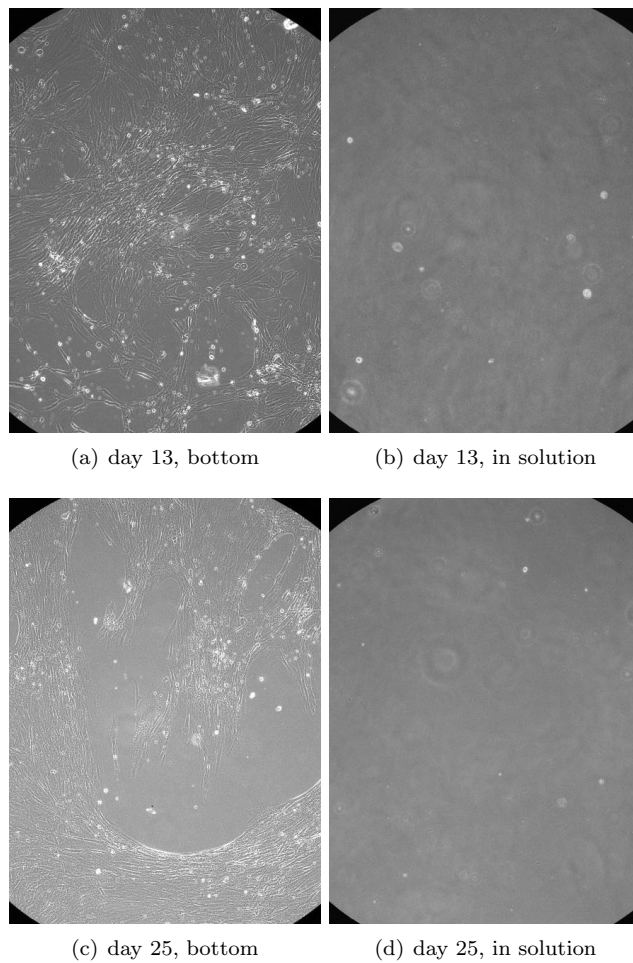


Figure 4.7: **Spontaneous differentiation of ASCs.** *Since some cells adhered to the bottom of the culture plates and some ASCs stayed in the solution, images of both populations were obtained. The morphology of ASCs maintained in the solution was round and it did not change throughout the period of culturing. The adherent ASCs developed these tube-like structures.*

Due to the viscous properties of the applied medium, a fraction of ASCs

were maintained in the solution and the images depicted in Fig.(4.7) show that the morphology of the cells did not change throughout the 26 days of culturing. This does not indicate that the ASCs have initiated spontaneous differentiation toward the cardiomyogenic lineage. The use of normal PST culture plates allowed the ASCs to adhere to the bottom and as illustrated in Fig.(4.7), the ASCs developed a tube-like network. Based on these observations, the expression of the early endothelial markers, VWF and VEGFR-2, was also investigated. The results from the real-time PCR analysis are illustrated in Fig.(4.8) and the expression of the markers was normalized to ASCs cultured in normal growth medium and on PST. The ASCs that stayed in the solution showed no expression of MEF2C and GATA-4 and the expression of MEF2C was also down-regulated in ASCs that adhered to the bottom. The expression of VEGFR-2 was up-regulated in ASCs maintained in solution and in adherent day 13 ASCs. However, at day 26 no difference in expression was observed between the control ASCs and the adherent day 26 ASCs. VWF and VEGFR-2 were up-regulated around 1000 times in the positive control, which was far more than the up-regulation observed in adherent day 13 ASCs. This indicates that the ASCs, which developed these tube-like structures, were not endothelial progenitor cells.

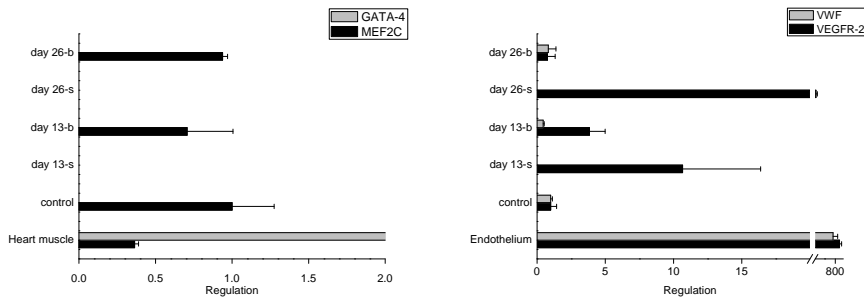


Figure 4.8: **Expression of cardiac and endothelial markers.** *The expression of cardiac- and endothelial markers was normalized to ASCs cultured in normal growth medium and on PST. No expression of MEF2C and GATA-4 was observed in the non-adherent ASCs, and the expression of MEF2C was furthermore down-regulated in adherent ASCs. VEGFR-2 was up-regulated in non-adherent ASCs at both day 13 and day 26 and adherent ASCs at day 13, however, no expression or a down-regulation of VWF was observed. VWF and VEGFR-2 were up-regulated around 1000 times in the positive control, which is far more than the up-regulation observed in adherent day 13 ASCs.*

Since the first protocol did not produce any promising results, a second protocol was developed and this protocol combined the methylcellulose-based medium with both AZA and ZEB. P1 and P8 ASCs were mixed with the methylcellulose-based medium and AZA and ZEB were added to the solution. Since it was impossible to change the medium, the ASCs were exposed to AZA and ZEB for the entire period of culturing. The ASCs were again divided into two lysis samples as both adherent and non-adherent ASCs were observed. The expression profile is illustrated in Fig.(4.9) and none of the ASCs expressed GATA-4 and the expression of MEF2C was not up-regulated compared to the

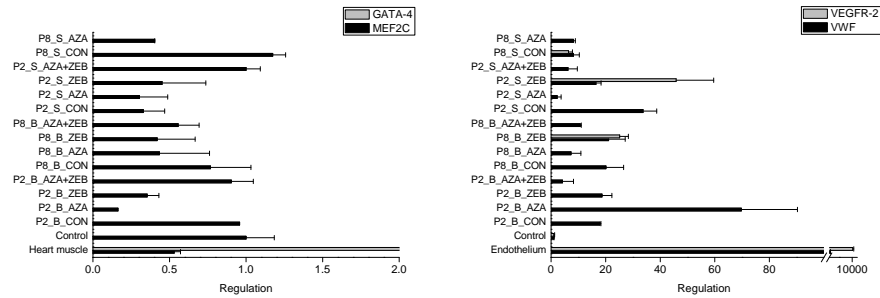


Figure 4.9: **Expression of cardiac and endothelial markers.** *The expression of cardiac- and endothelial markers was normalized to ASCs cultured in normal growth medium and on PST. No expression of GATA-4 was observed and the expression of MEF2C was not up-regulated compared to the control ASCs. VWF was expressed in all samples, whereas VEGFR-2 was only expressed in a few samples. Compared to the control, VWF in VEGFR-2 were up-regulated in the samples but the up-regulation of VWF and VEGFR-2 was even greater in the positive control.*

control cells. VWF was expressed in all samples, whereas VEGFR-2 was only expressed in a few samples. Compared to the control, VWF in VEGFR-2 were up-regulated in the samples but the up-regulation of VWF and VEGFR-2 was even greater in the positive control. The difference in up-regulation indicates that the combined treatment of methylcellulose-based medium and the chemical inducers did not initiate any differentiation of ASCs.

AZA has been shown to initiate expression of silenced genes in cancer cells and it could therefore be of interest to determine if the combined treatment of methylcellulose-based medium and AZA and ZEB could induce differentiation along other lineages than the cardiomyogenic and endothelial. Expression of markers of cardiac muscle-, endothelial-, nervous-, skeletal muscle-, cartilage-, bone- and adipose tissue was therefore investigated. The results are depicted in Fig.(4.10). MYOD1 was up-regulated in S_ZEB and S_AZA compared to the control ASCs, however, MYOD1 was up-regulated over 4000 times in the positive control compared to the control ASCs. It is therefore very unlikely that the S_AZA and S_ZEB ASCs have initiated differentiation. The expression of NES was up-regulated around 3 times in B_AZA but no expression of NGFR was observed. The expression of NES in the positive control was 30 times as high as the control ASCs and the B_AZA ASCs have therefore not developed into neurogenic progenitor cells. COL2A1 was up-regulated in the B_Control ASCs but the expression of SOX9 was though down-regulated and an up-regulation of SOX9 would be expected if the B_Control ASCs have developed toward the chondrogenic lineage. No up-regulation of ONN and CBF α 1 was observed. The expression of AP2 was up-regulated in all ASCs maintained in solution but the expression of PPAR γ 2 was down-regulated. The addition of methylcellulose changes the medium to a gel, which is very soft and with a low YM. The ASCs will react on the elastic properties of the gel and the response can be differentiation. Adipose tissue also has a very low YM and this could explain the up-regulation of AP2. It should be noted that the up-regulation of AP2 was even greater in the positive control.

4.3. RESPONSE TO CULTURING IN METHYLCELLULOSE-BASED MEDIUM

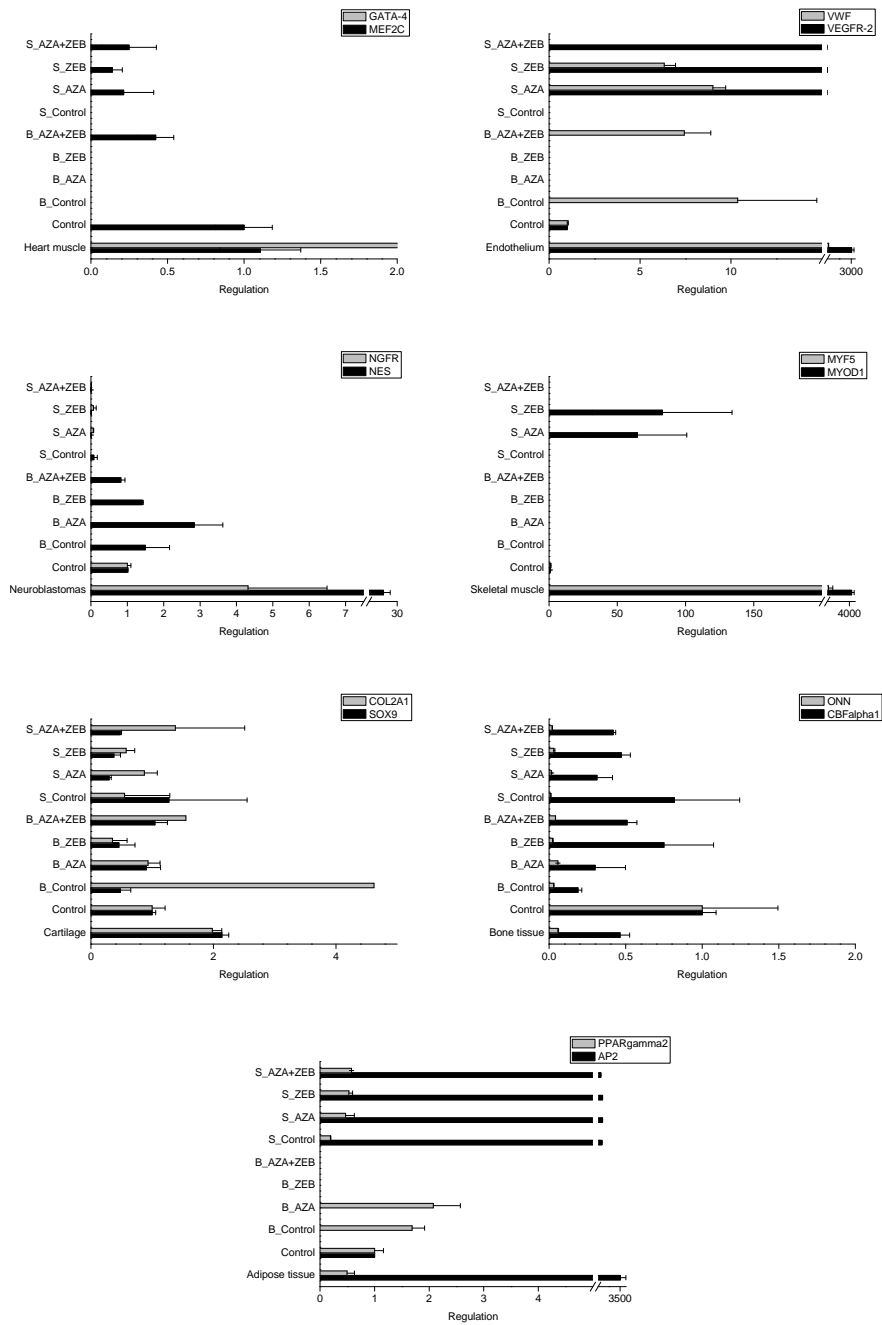


Figure 4.10: **Gene assay expression.** Expression of markers of cardiac muscle-, endothelial-, nervous-, skeletal muscle-, cartilage-, bone- and adipose tissue was investigated. The expression of AP2 was up-regulated in all ASCs maintained in solution but the expression of PPAR γ 2 was down-regulated. The addition of methylcellulose changes the medium to a gel, which is very soft and with a low YM. The ASCs will react on the elastic properties of the gel and the response can be differentiation.

4.4 Response to 5-azacytidine and Zebularine Treatment

P1 ASCs were used to determine the optimal concentration of both AZA and ZEB. ASCs were seeded at 1000 cells/cm² and cultured in normal growth medium for 24 hours. Based on the studies described in Sec.(1.4) the concentration of AZA and ZEB varied between 1 and 20 μ M. After 24 hours of culturing, the induction medium was added. Medium both with and without FCS was used. A selection PCM images obtained after day 13 are depicted in Fig.(4.11). After 13 days the ASCs have reached completed confluency independent of the inducer added and the concentration of the inducer. The morphology of the induced cells have not changed compared to the control during the 13 days of culturing and suggest that neither AZA nor ZEB induced differentiation of the ASCs.

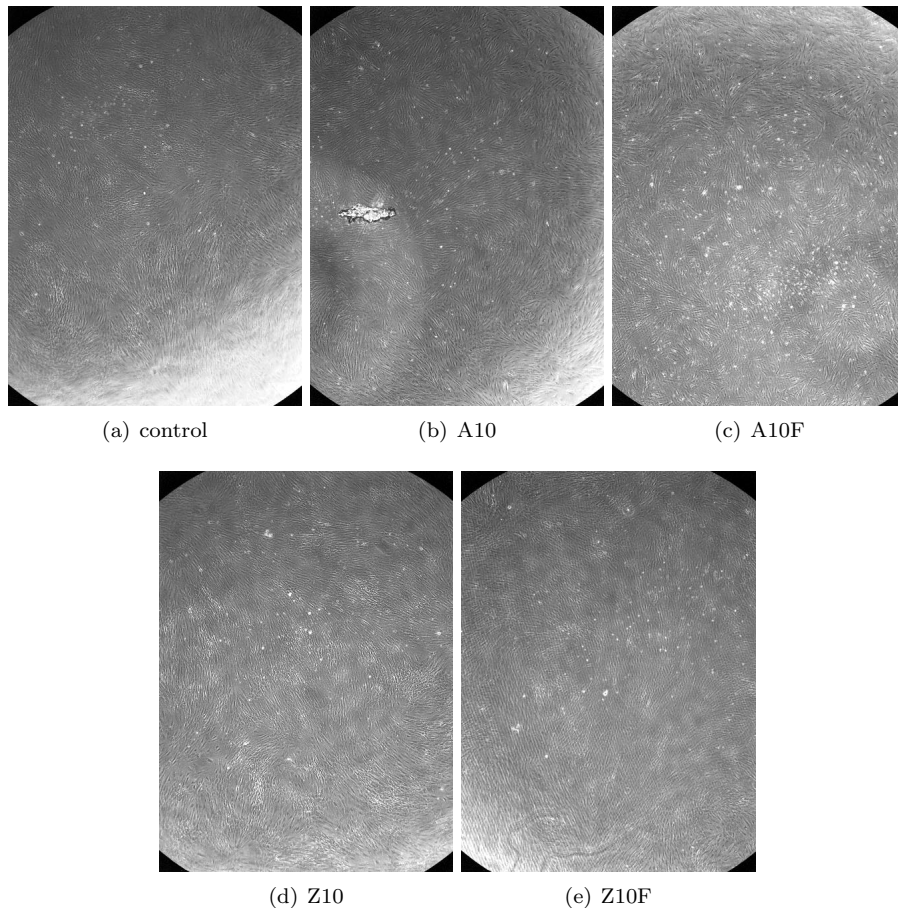


Figure 4.11: A selection of PCM images of ASCs induced with AZA and ZEB. A and Z are abbreviations for AZA and ZEB, respectively. The number indicates the concentration of inducer added to the ASCs and F indicates the use of FCS. The images were obtained after 13 days of culturing. The morphology of the ASCs does not indicate that the cells have developed toward the cardiomyogenic lineage.

In order to verify that the ASCs induced with AZA and ZEB have not developed toward the cardiomyogenic lineage, the expression of GATAA-4 and MEF2C was investigated and the results are depicted in Fig.(4.12). The expression was normalized to ASCs cultured on normal tissue culture plates and no expression of GATA-4 was detected. MEF2C was expressed in all samples, however the maximum up-regulation was 1.5 and compared to the expression of MEF2C in the positive control, this up-regulation is insignificant.

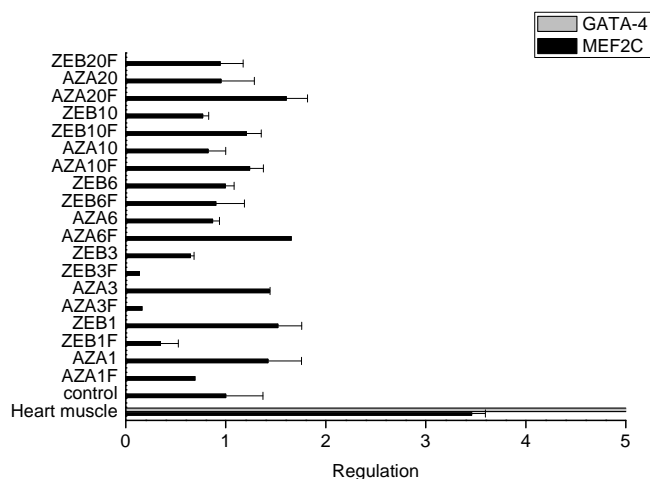


Figure 4.12: **Expression of MEF2C and GATA-4 in ASCs induced with different concentration of AZA and ZEB.** The expression of MEF2C and GATA-4 was normalized to the control, which was ASCs cultured on a normal tissue culture plate. The results show that the induced ASCs did not express GATA-4 and that the expression of MEF2C was not significantly up-regulated

Since the PCM images and the real-time PCR results indicated that the 24 hour treatment with different concentration of AZA and ZEB did not guide the ASCs toward the cardiomyogenic lineage, another experiment was set up. In stead of treating the P1 ASCs for 24 hours, the cells were treated continuously with AZA or ZEB. Instead of only investigating if the ASCs expressed cardiac markers, it could be of interest to investigate the expression of early markers of tissues from all three germ layers. It has been proved that AZA can induce expression of several genes in tumor cells [31]. Expression of markers of cardiac muscle-, endothelial-, nervous-, skeletal muscle-, cartilage-, bone- and adipose tissue was therefore investigated. The results are depicted in Fig.(4.13).

No expression of GATA-4 was observed and the expression of MEF2C was down-regulated compared to both the control and the positive control. The continuous treatment of ASCs with AZA and ZEB did not trigger any cardiomyogenic differentiation. It though seemed like AZA and ZEB influenced the expression of early markers of both skeletal muscle- and nervous tissue. MYOD1 and MYF5 were up-regulated around 60 times in the AZA treated ASCs. However, MYOD1 and MYF5 were up-regulated 4000 and 1000 times, respectively, and this means that it is very unlikely that the AZA treated ASCs have initiated differentiation. This was also verified by the lack of MYOD1

expression in the AZA and ZEB treated ASCs. The real-time PCR results also show that the expression of the nervous tissue markers, NES and NGFR, was up-regulated compared to the control ASCs. The expression of NES in the positive control was still much higher compared to the induced cells. However, the expression of NGFR was also up-regulated compared to the positive control. The AZA treatment induced a higher expression of both NES and NGFR compared to the ZEB treatment, but a treatment with both AZA and ZEB induced the highest expression levels compared to the other two treatments.

4.4. RESPONSE TO 5-AZACYTIDINE AND ZEBULARINE TREATMENT

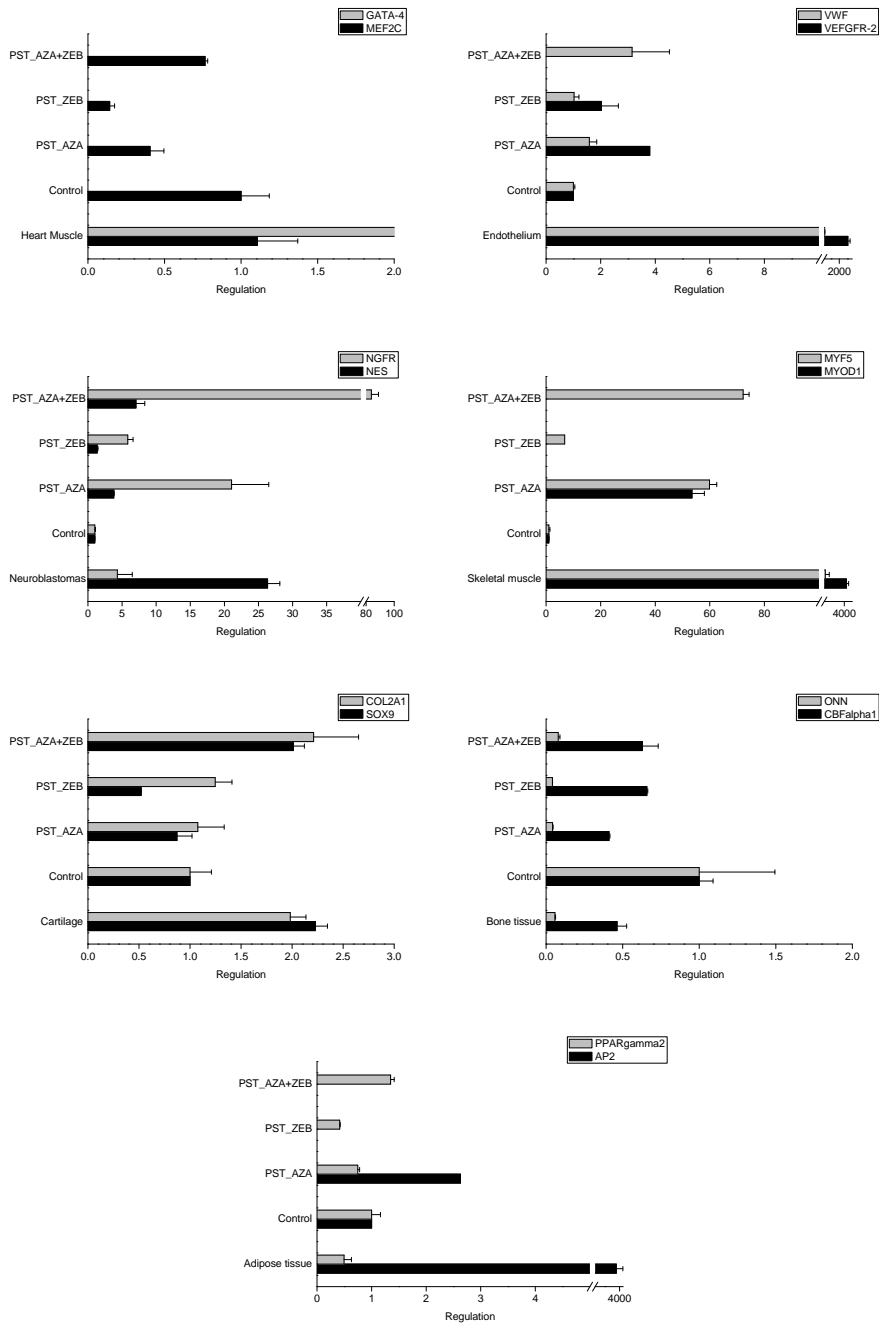


Figure 4.13: **Gene assay expression** Expression of markers of cardiac muscle-, endothelial-, nervous-, skeletal muscle-, cartilage-, bone- and adipose tissue was investigated. The up-regulation of MYOD1 and MYF5 in the positive control proves that it is very unlikely that the ASCs had induced differentiation toward the myogenic lineage. An up-regulation of NGFR was observed, also compared to the positive control, and the combined treatment of AZA and ZEB induced the highest expression level of NGFR.

Chapter 5

Discussion

5.1 Influence of Matrix Elasticity on Cell Behavior

Based on the immunocytochemical analysis and the preliminary experiment described in Sec.(4.2), it was established that the sulfo-SANPAH mediated crosslinking could not be used. This results is in strong contrast with literature as sulfo-SANPAH by far is the most applied crosslinker used in relation to PA gels [15, 16, 19, 53, 65, 66, 67, 68]. Even though the use of sulfo-SANPAH has been extensively described in the literature, it has several drawbacks. It is very unstable both when stored and when dissolved in a buffer. Another explanation to the lack of crosslinked COLI and FIB, which is shown in Fig.(4.1E,F), is that the sulfo-SANPAH used in this project was ordered from another company compared to the references.

When applying sulfo-SANPAH, it is necessary to go through several steps including ultraviolet crosslinking. The wavelength of the incident light varies in the literature. Engler and co-workers [51] used incident light with a wavelength of 365 *nm*, whereas the material data sheet [69] states that the photolysis should be performed with UV light with a wavelength within 320-350 *nm*. An article published by Ideno et al. [70] describe the use of 312 *nm* light to activate sulfo-SANPAH. The variation in the wavelength of the incident light suggests that sulfo-SANPAH can be activated by a broad spectra of light in the UV range and the use 340-385 *nm* UV light should therefore be sufficient. The distance between sample and light source, the intensity of the light and the exposure time could also influence the crosslinking. The literature suggests that the working distance can vary between 5 and 15 *cm* without influencing the crosslinking. Ideno et al. [70] applied a working distance of 5 *cm* and an exposure time of 15 *min*, whereas Pelham et al. [15] applied a working distance of 15 *cm* and an exposure time of 5 *min*. This setup has also been used by Engler et al. [19, 51, 52], Yeung et al. [16] and Deroanne et al. [53]. These references have all had success with sulfo-SANPAH and sulfo-SANPAH can therefore be activated by using different setups. Sulfo-SANPAH from different manufacturers should be tested while applying the same light source, exposure time and working distance.

Two other methods were then tested and the EDC/NHS mediated crosslink-

ing proved to efficiently crosslink both COLI and FIB to the PA gels, whereas the glutaraldehyde mediated crosslinking did not produce the same uniform layer of neither COLI nor FIB. A preliminary experiment was setup in order to investigate if ASCs could spread on COLI and FIB crosslinked PA gels. Fig.(4.4G,H) show that the ASCs could spread on PA gels where EDC/NHS has been applied. The result is not included in this thesis but after four days of culturing in normal growth medium, the ASCs cultured on the COLI crosslinked PA gel had reached confluency. Fig.(4.4C,D) show that ASC cultured on PA gels where glutaraldehyde crosslinking has been applied, do not spread but maintain their round morphology. Glutaraldehyde is a toxic chemical that can be used for fixation of cells and it is therefore important to thoroughly wash the gels before use. The addition of ASCs suspended in normal growth medium proved that glutaraldehyde was present in the gel as the medium changed color from red to yellow.

P1 ASCs were then cultured on both COLI and FIB crosslinked PA gels resembling nervous, muscle- and bone tissue. The ASCs were cultured for 14 days and PCM images were obtained during the period of culturing. The morphology of ASCs cultured on the soft COLI crosslinked PA gel was round, as seen in Fig.(4.5A), whereas ASCs cultured on the the harder gels were more elongated, as seen in Fig.(4.5B,C). A study performed by Wang et al. [71] showed that fibroblast react on substrate elasticity. An increase in cell apoptosis and a decrease in DNA synthesis were observed in fibroblasts that were cultured on a soft substrates. This response was coupled to a decrease on cell spreading area of the fibroblasts. Yeung et al. [16] also found that spreading of fibroblasts was dependent on substrate elasticity, however, the same study also investigated how neutrophils react on substrate stiffness and the results showed that these cells spread equally well on both soft and hard substrates. In general, the response on substrate stiffness depend on the cell type and since ASCs have almost the same phenotypic profile as bmMSCs, it was expected that the ASCs would spread on the three different PA gels and develop tissue specific morphologies. Engler et al. [19] found that bmMSCs from humans both express tissue specific markers and spread on COLI crosslinked PA gels. After four hours of culturing, a difference in cell morphology was observed and the morphologies were dependent on matrix elasticity. Fig.(4.5D) depicts that ASCs on the soft PA gels were more elongated at day 6 compared to day 2. The morphology of these ASCs does not differ from ASCs cultured on the more stiff substrates, as seen in Fig.(4.5E,F). Yeung et al. [16] also investigated the change in morphology of endothelial cells cultured on substrates with increasing elasticities. The morphology of endothelial cells cultured on a 180 *Pa* gel was round after one day of culturing, whereas endothelial cells on 2900 *Pa* and 29000 *Pa* gels were elongated. After three days of culturing it proved impossible to distinguish between the endothelial cells cultured on the different gels. They propose that this could be explained by contact between the cells. The contact between cells was very limited on all the PA gels as the cells did not proliferate and it thus seem like the ASCs need more time to adapt to very soft substrates.

The morphology of the ASCs cultured on the FIB crosslinked PA gels showed similar trends as the ASCs cultured on the COLI substrates. As illustrated in Fig.(4.6A,D,H) the morphology of the ASCs cultured on the soft surface does not change throughout the entire period of culturing. Very soft substrates can induce apoptosis due to no cell adhesion and spreading [14], but this does

not comply with the cell spreading observed on the soft COLI substrate. A study performed by Engler and co-workers [51] showed that the concentration of crosslinked COLI influence the spreading of smooth muscle cells. The lack of ASC spreading could be explained by a too low concentration of FIB on the PA gel. The ASCs cultured on the two stiff substrates spread and the ASCs were elongated, as seen in Fig.(4.6B,C,E,F,H,I).

Based on the preliminary experiment, it was expected that the ASCs would reach confluency after 14 days of culturing. This was not the case and the explanation could be related to the fabrication of the gels. The application of EDC/NHS to crosslink proteins to PA gels have not yet been described, however, Hofman et al. [72] studied the effect of different scaffolds on bmMSCs proliferation. They observed that bmMSCs could proliferate on scaffolds where EDC/NHS has been used as the crosslinking agent. The PCM images do not indicate that an fungi infection has been introduced to the culture and the production of the gels also involve a exposure to UV light immediately before adding the EDC/NHS solution. The ASCs could also have been contaminated by bacteria or mycoplasma. A mycoplasma contamination can influence the metabolic activity and proliferation of cells [73, 74, 75]. However, the ASC cell line used for the experiment has been tested for mycoplasma contamination. Any contamination would have been introduced during the production of the PA gels.

It does not seem like there, apart from the soft substrates, was any difference in cell behavior between the COLI- and FIB crosslinked PA gels. The experiment was setup in order to determine if any ASCs had initiated differentiation but it proved impossible to extract enough RNA for further real-time PCR analysis. This was due to a combination of a low cell culturing area and a low cell density. Further experiments should focus on the fabrication of COLI and FIB crosslinked PA gels.

5.2 Matrix Elasticity

The elasticity of the PA gels can be altered by a change in AM- and MBA concentration. In order to produce PA gels with YM that resemble nervous-muscle- and bone tissue, it is necessary to determine the YM of the gels. AFM measurements were used in this project and the results show that the YM of PA gels increases when the concentration of MBA also increases. This results complies with results published by both Engler et al. [51], Pelham et al. [15] and Boudou et al. [57]. Boudou and co-workers [57] determined the YM of PA gels made from 10% AM solutions and their calculations showed a higher YM and the difference was at least 2-fold. The reason for this difference could be the use of another method to determine YM of the gels. They used images of the indentation of micropipettes in the PA gels and the calculation of YM was based on an extension of Theret's relationship instead of the Hertzian models.

The addition of AA to the AM solution was necessary when applying the EDC/NHS crosslinking method as EDC crosslinks amino- and carboxylic acid groups. The YM values in Tab.(4.1) show that the addition of AA increased the YM of the PA gels compared to PA gels without AA. Since AA binds to MBA by the same reaction as AM, it was not expected that the YM would increase. It was possible to produce PA gels possessing elastic properties that

resembled nervous-, muscle and bone tissue, however, the calculations of the YM was only based on measurements performed on only one gel. In order to produce reliable results, AFM measurements on more gels should be conducted. Boudou and co-workers [57] have also shown that YM of PA gels, made from the same solution, varies as much as 30 kPa . In addition to the determination of YM, it was investigated if the amount of crosslinked protein would change when the elasticity change. This was done by measuring the relative amount of COLI crosslinked to the three different PA gels applied for the ASC differentiation experiment. Fig.(4.3) show that there was a significant difference in the amount of COLI crosslinked between the three PA gels. The amount of crosslinked decreases when the stiffness increases. Engler et al. [51] found that the amount of protein crosslinked to the surface influence the spread cell area. The cell area was constant when the cells were cultured on COLI concentrations between 100 and 5000 10 ng/cm^2 but very low (10 ng/cm^2) and very high concentrations ($100,000 \text{ ng/cm}^2$) of COLI gave rise to a decrease in cell area. It is therefore of interest to construct gels crosslinked with the same amount of COLI and FIB in order to investigate the effect of matrix elasticity on cell behavior.

5.3 Spontaneous Differentiation

Both Palpant et al. [47] and Planat-Benard et al. have proved that mouse adipose derived SCs spontaneously differentiate into beating cells when cultured in a methylcellulose-based medium intended for hematopoietic SCs. Fig.(4.7A) show that the use of normal PST culture plates allow for cell adhesion and that the ASCs spread. During the period of culturing the ASCs developed endothelial-like networks, as seen in Fig.(4.7C,E). Even though some ASCs adhered to the bottom, it was still possible to locate ASCs in the solution. Fig.(4.7B,D,F) show that the morphology of the ASCs does not change throughout the period of culturing. Planat-Benard and co-workers [46] observed that the mouse adipose derived SCs developed into elongated cells after 17 days and after 24 days in culture the cells had initiated simultaneous contraction.

Based on the images in Fig.(4.7B,D,F) the ASCs did not develop toward the cardiomyogenic lineage, however, a real-time PCR analysis was performed in order to determine if the ASCs that stayed in the medium expressed GATA-4 and MEF2C. Fig.(4.8) show that the ASCs did not express any GATA-4 and that the expression of MEF2C was down-regulated compared to the control ASCs. The expression of MEF2C was also down-regulated in the positive control and this suggest that the human cardiomyocytes used for the extraction of positive RNA were to mature. Planat-Benard et al. [46] also showed that the beating cells did express several cardiac markers including GATA-4 and NKX2.5. Palpant et al. [47] did not investigate the expression of GATA-4 or MEF2C but they still observed expression of several other cardiac markers including cardiac troponin I. Fig.(4.8) also show that VEGFR-2 was up-regulated in all samples except day 26-b. VWF was on the other hand not expressed in neither day 13-s nor day 26-s and the expression of VWF in the day 13-b and day 26-b ASCs was down-regulated. VWF and VEGFR-2 were up-regulated around 800 times in the positive control, as seen in Fig.(4.8). It was not expected that ASCs in solution would express any endothelial markers and since no VWF expression was detected, it is very unlikely that these ASCs had developed into endothelial

precursor cells. The adherent ASCs expressed both VWF and VEGFR-2 at day 13 and the expression of VEGFR-2 was up-regulated. At day 26 the expression of both VWF and VEGFR-2 was down-regulated in the adherent ASCs. It is also unlikely that these ASCs had initiated any differentiation.

A combination between a chemical treatment with AZA and ZEB and the use of the methylcellulose-based medium was therefore investigated. The adherent ASCs also developed this endothelial-like network while the ASCs in solution maintained their round morphology. Both P2 and P8 ASCs were used in this experiment. Fig.(4.10) show the expression of early cardiac- and endothelial markers. No expression of GATA-4 was observed after 13 days of culturing and the MEF2C expression in the ASCs was either down-regulated or comparable to the control ASCs. VWF was expressed in all ASC samples and furthermore up-regulated compared to the control ASCs. Even though VWF was up-regulated between 5 and 70 times, the expression levels were still very low compared to the positive control. VEGFR-2 was not expressed in all the ASC samples, but it was up-regulated in the P8_S_CON, P2_S_ZEB and P8_B_ZEB ASCs. There was no coherence between these samples as both adherent ASCs and ASCs in solution expressed VEGFR-2. The up-regulation of VEGFR-2 was also very low compared to the up-regulation in the positive control. The methylcellulose-based medium contains growth factors normally used for differentiation toward the hematopoietic lineage. These growth factors are interleukin 3, interleukin 6 and stem cell factor. Palpant et al. [47] investigated if these growth factors influence the differentiation into beating cells and they observed a significant higher number of beating colonies when growth factors were added to the medium.

Since AZA has proved to induce expression of several genes in cancer cells, the expression of specific markers of cardiac muscle-, endothelial-, nervous-, skeletal muscle-, cartilage-, bone- and adipose tissue was investigated. The expression profile is illustrated in Fig.(4.10). It is first of all important to notice that the standard deviation of gene regulation, in many cases, was very high. The real-time PCR analysis was based on duplicates and the standard deviation should be very low. An explanation could be poor pipetting, but this explanation does not seem reasonable as the standard deviation of gene regulation in the control ASCs was not pronounced. The experiment was setup in a 24-well plate and this reduced the amount of RNA. A low concentration of RNA can lead to high standard deviations as the expression level was near the detection limit of the equipment [76]. The gene assay did not give any unambiguous results, however, the expression of AP2 in ASCs maintained in the solution was up-regulated approximately 600 times compared to the control ASCs. Since the S_Control ASCs also up-regulated the expression of AP2, AZA and ZEB did not seem to influence the AP2 expression. The medium had gel-like properties due to methylcellulose and since elasticity can affect the differentiation of SCs, it could be the elastic properties of the medium that induced the expression of AP2. Since adipose tissue is very soft and has a YM of around 2000 Pa [77, 78], the methylcellulose-based medium could induce differentiation toward the adipogenic lineage. No up-regulation of PPAR γ 2 was though observed and since PPAR γ 2 has been identified as a regulator of AP2 it would be expected that an up-regulation of PPAR γ 2 would have been observed as well [79, 80]. The elastic modulus of nervous tissue is even lower than the elastic modulus of adipose tissue, but both NES and NGFR were down-regulated in the ASCs maintained in the methylcellulose-based medium.

5.4 5-azacytidine and Zebularine Treatment

A preliminary experiment was setup in order to determine the optimal concentration of AZA and ZEB. After 13 days of culturing, PCM images were obtained and RNA was extracted. Fig.(4.11) show that the morphology of the induced ASCs did not change compared to ASCs cultured in normal growth medium and on PST culture plates. The expression of GATA-4 and MEF2C was examined and Fig.(4.12) shows that the ASCs did not differentiate toward the cardiomyogenic lineage. Based on this experiment it was very difficult to determine the most suitable concentration of AZA and ZEB as the result suggests that AZA and ZEB do not influence the expression of early cardiac markers. Several studies have investigated the effect of AZA and proved that human bmMSCs and umbilical cord derived MSCs express early cardiac markers and develop cardiomyocyte features [34, 35, 36]. The published material of these studies does not state how many experiments were made in order to successfully guide the SCs toward the cardiomyogenic lineage. Since activation of genes through AZA treatment is somewhat random, it is hard to believe that the success rate of these studies was 100%. Liu et al. [42] exposed rat bmMSCs to three different concentration of AZA and the cells did not express any early cardiac markers after the period of culturing. A more recent study performed by Lee and co-workers [81] show that human ASCs did not express NKX2.5 and GATA-4 after treatment with AZA. The cells were treated with two different concentrations of AZA (5 and 10 μM) for 24 *h* or repeatedly through eight weeks of culturing.

A second experiment was setup in order to determine if a combined treatment of AZA and ZEB could influence the gene expression in ASCs. A concentration of 10 μM was used for both AZA and ZEB. In stead of only investigating the expression of GATA-4 and MEF2C, the expression of an array of genes was investigated since AZA has shown to induce the expression of several genes in cancer cells [31]. Fig.(4.13) depicts the expression of specific markers of cardiac muscle-, endothelial-, nervous-, skeletal muscle-, cartilage-, bone- and adipose tissue. GATA-4 was not expressed and the expression of MEF2C was down-regulated compared to the control ASCs and the positive control. Christman et al. [31] reported that the expression of MYOD1 was initiated in cancer cells treated with AZA. Interestingly, the expression of both MYOD1 and MYF5 were up-regulated in the PST_AZA ASCs but a comparison to the positive control show that this up-regulation was very low. However, NES and NGFR were up-regulated in PST_AZA, PST_ZEB and PST_AZA+ZEB and the NGFR expression was even up-regulated compared to the positive control. A further analysis of the expression of neurogenic markers is needed in order to verify this result. Other methods to induce neurogenic differentiation of ASCs have already been described. Safford et al. [82] used induction medium containing valproic acid, hydrocortisone, insulin and forskolin, among others, and immunocytochemical analysis proved that the ASCs expressed NES and NeuN. A pre-treatment with EGF (epithelial growth factor) and FGF enhanced the protein expression. Anghileri and co-workers [83] also applied this pre-treatment before adding induction medium, containing retinoic acid and brain-derived neurotrophic factor, to the ASCs. Expression of neurogenic markers was also observed. Since other methods to induce differentiation of ASCs into neuron-like cells have been described, it would not be reasonable to examine the effect of AZA and ZEB in regard to neurogenic differentiation. The reactivation

of silenced genes by AZA and/or ZEB treatment is somewhat random and it is of interest to develop protocols that have a high success rate.

5.5 Experiment Improvements

It is first of all necessary to address the COLI and FIB crosslinked PA gels, since the ASCs did not proliferate on the substrates. Even though the preparation of the gels involve a sterilization step, the PA gels should be washed several times with an ethanol solution even though it will difficult to wash out the ethanol. This should definitely prevent any contamination before the ASCs are seeded on the gels. It proved difficult to obtain enough RNA for real-time PCR and this can be improved by increasing the starting cell density and the area of cell culturing. Another improvement is related to the elasticity calculations. These are only based on single measurement and in order to obtain a reliable results, several samples should be prepared of the same AM solution and furthermore several measurements should be performed on each sample. This will also make it possible to determine if the force plots obtained by AFM measurements are useful for determining the YM of the gels.

The chemical treatments of ASCs with AZA are based on information found in several references and so far various setups have been described. It is very difficult to determine the success rates of AZA treatments and it could therefore be of interest to setup a large scale experiment In this experiment, the differentiation of ASCs and mouse adipose derived stem cells should be investigated. The application of ZEB in regard to differentiation toward the cardiomyogenic lineage has not yet been described, however, ZEB has been used to transdifferentiate mouse myoblasts into smooth muscle cells [44]. The concentration of ZEB in this study was either 25 μM or 100 μM . It could therefore be of interest to investigate if an increased concentration of ZEB could influence the gene expression in ASCs.

In general, real-time PCR is associated with several sources of errors and the standard deviations also prove that the real-time PCR analysis should be improved. The concentration of RNA obtained after cell lysis of the control ASCs cultured on PST was very high compared to the concentration of RNA extracted from the other samples. This difference could explain the low standard deviations of gene expression of the control ASCs, likewise the high standard deviations of gene expression of most of the other samples. According to [76], a low RNA concentration can lead to high standard deviations, as the total amount of amplified DNA is near the detection limit of the equipment. It is possible to obtain a higher concentration of RNA by increasing the area of cell culturing. Another improvement related to real-time PCR is the selection of primers. Two specific primers for each type of tissue were chosen and more primers could be used in order to make to real-time PCR analysis more specific. An example of a primer that can be expressed in more than one tissue is MEF2C, which is involved in both cardiomyogenesis and neurogenesis.

Chapter 6

Conclusions

The characterization of COLI and FIB crosslinked PA gels showed that the EDC/NHS mediated crosslinking generates the most uniform layer of protein. The preliminary experiment proved that ASCs could spread and proliferate on PA gels where EDC/NHS was used as the crosslinker. However, the final experiment setup to investigate the differentiation of ASCs indicated that effort has to be put into the fabrication of the gels as the ASCs did not proliferate.

The application of a methylcellulose-based medium to guide the ASCs toward the cardiomyogenic lineage did not have any effect on the expression of GATA-4 and MEF2C. The real-time PCR analysis proved that the adherent ASCs had not developed into endothelial-like cells. A combined treatment of AZA and ZEB and the methylcellulose-based medium was therefore examined. Both the PCM images and the real-time PCR analysis showed that this treatment did not induce any differentiation toward the cardiomyogenic- or other lineages.

The addition of AZA and ZEB to normal growth medium did not cause any change in GATA-4 and MEF2C gene expression. ASCs exposed to AZA and ZEB as well as a combined treatment of the two chemicals were analyzed in regard to the designed gene assay and the expression of NGFR was up-regulated compared to both the control ASCs and the positive control. Furthermore, the up-regulation was highest in ASCs induced with AZA and then ZEB. A more thorough investigation of gene- and protein expression has to be performed to verify this result.

In conclusion, the treatment of ASCs with AZA and ZEB as well as the use of a methylcellulose-based medium can not be used to induce differentiation of ASCs into cardiomyocyte-like cells. In stead the use of PA gels crosslinked with ECM proteins makes it possible to mimic the elastic properties of the tissues in the human body. A combination between these substrates and appropriate growth factors could trigger differentiation by influencing the signaling pathways in the ASCs and thereby trigger differentiation.

Chapter 7

Perspectives

Before actually investigating the differentiation of ASCs cultured on the different gels, it could be of interest to perform both cell spreading and cell proliferation experiments. It is very difficult to conclude anything regarding area and proliferation based on PCM images. These experiments will also contribute to increase the knowledge regarding mechanosensing of cells in general and more interestingly, the mechanosensing of ASCs.

In stead of adding AZA and ZEB to the methylcellulose medium and normal growth medium it could be of interest to investigate the effect of growth factors or substances that influence the different signaling pathways involved in cardiomyogenesis. The BMP and FGF signaling pathways are involved in cardiomyogenesis. As described in Sec.(1.3) studies have shown that the myocardium contain high amounts of FGF-2 in the early stages of cardiomyogenesis. Bartunek et al. [84] found that human bmMSCs express early cardiac markers after 3 weeks of culturing in a differentiation medium containing ascorbic acid and human leukemia inhibitory factor, among others, followed by a 6 day FGF, BMP-2 and IGF (insulin-like growth factor 1) treatment. The morphology of the human bmMSCs did not change after the treatment and this also verifies that it is necessary to examine the transcriptional regulation of cells in order to determine if they have initiated differentiation. It has furthermore been shown by Kawai et al. [85] that a BMP and FGF-2 treatment of embryoid bodies enhance the expression of NKX2.5 and actinin.

ASCs are now cultured on PST culture plates, which has a very high YM compared to the different tissues in the human body and it is therefore a non physiological environment. PA gels offer a possibility to mimic the elasticity of the tissues and it is furthermore possible to crosslink ECM proteins to the gels by using EDC/NHS. PA gels are also inert and transparent and this makes it possible to monitor the development of the cells. It has been shown that both transforming growth factor- β and mechanical tension are critical for the differentiation of rat fibroblasts into myofibroblasts [86, 87]. A combination between substrates with different elasticities and the use of suitable growth factors could be used to guide the differentiation of ASCs while culturing them on substrates that has similar properties of tissues in the human body.

Bibliography

- [1] Department of Health and Human Services. *Stem Cells: Scientific Progress and Future Research Directions*, June 2001. <http://stemcells.nih.gov/info/scireport/2001report>.
- [2] Thomson J., Itskovitz-Eldor J., Shapiro S., Waknitz M., Swiergiel J., Marshall V., and Jones J. Embryonic stem cell lines derived from human blastocysts. *Science*, 282(5391):1145–1147, 1998.
- [3] Department of Health and Human Services. *Stem Cell Basics*, 2006. <http://stemcells.nih.gov/info/basics/basics1>.
- [4] The National Academy of Sciences. *Understanding Stem Cells*, 2006. <http://dels.nas.edu/bls/stemcells/basics.shtml>.
- [5] Minguell J. J., Erices A., and Conget P. Mesenchymal stem cells. *Experimental Biology and Medicine*, 226(6):507–520, 2001.
- [6] Caplan A.I. and Bruder S.P. Mesenchymal stem cells: building blocks for molecular medicine in the 21st century. *Trends in Molecular Medicine*, 7(6):259–264, June 2001.
- [7] Meirelles L.d.S and Nardi N.B. Methodology, biology and clinical applications of mesenchymal stem cells. *Frontiers in Bioscience*, 14:4281–4298, January 2009.
- [8] Pountos I., Corscadden D., Emery P., and Giannoudis P. Mesenchymal stem cell tissue engineering: Techniques for isolation, expansion and application. *Injury, Int. J. Care Injured*, 38(4):23–33, September 2007.
- [9] Tuan R. S., Boland G., and Tuli R. Adult mesenchymal stem cells and cell-based tissue engineering. *Arthritis Research and Therapy*, 5(1):32–45, December 2002.
- [10] Tapp H., Hanley E.N., Patt J.C., and Gruber H.E. Adipose-derived stem cells: Characterization and current application in orthopaedic tissue repair. *Experimental Biology and Medicine*, 234:1–9, 2009.
- [11] Zuk P.A., Zhu M., Ashjian P., Ugarte D.A.D, Huang J.I., Mizuno H., Alfonso Z.C., Fraser J.K., Behaim P., and Hedrick M.H. Human adipose tissue is a source of multipotent stem cells. *Molecular Biology of the Cell*, 13:42794295, December 2002.

- [12] Gimble J. M. and Guilak F. Adipose-derived adult stem cells: isolation, characterization, and differentiation potential. *Cytotherapy*, 5(5):362–369, 2003.
- [13] Lodish H., Berk A., Matsudaira P., Kaiser C. A., Krieger M., Scott M. P., Zipursky S. L., and Darnell J. *Molecular Cell Biology, 5th Ed.* Freeman, 2004.
- [14] Wells R.G. The role of matrix stiffness in regulating cell behavior. *Hepatology*, 47(4):1394–1400, 2008.
- [15] Pelham Jr R.J. and Wang Y. Cell locomotion and focal adhesions are regulated by substrate flexibility. *Proc. Natl. Acad. Sci.*, 94:13661–13665, 1997.
- [16] Yeung T., Georges P.C., Flanagan L.A., Marg B., Ortiz M., Funaki M., Zahir N., Ming W., Weaver V., and Janmey P.A. Effects of substrate stiffness on cell morphology, cytoskeletal structure, and adhesion. *Cell Motility and the Cytoskeleton*, 60:24–34, 2005.
- [17] Donald E. Ingber. Cellular mechanotransduction: putting all the pieces together again. *The FASEB Journal*, 20:811–827, 2006.
- [18] Discher D.E., Janmey P., and Wang Y.L. Tissue cells feel and respond to the stiffness of their substrate. *Science*, 310:1139–1143, 2005.
- [19] Engler A., Sen S., Sweeney H.L., and Discher D. Matrix elasticity directs stem cell lineage specification. *Cell*, 126:677–689, 2006.
- [20] Sadler T. W. *Langman’s Medical Embryology 10th Ed.* Lippincott Williams & Wilkins, 2006.
- [21] Brand T. Heart development: molecular insights into cardiac specification and early morphogenesis. *Developmental Biology*, 258:119, 2003.
- [22] Kirby M.L. Molecular embryogenesis of the heart. *Pediatric and Developmental Pathology*, 5:516543, 2002.
- [23] Zhu X. and Lough J. Expression of alternatively spliced and canonical basic fibroblast growth factor mRNAs in the early embryo and developing heart. *Dev. Dyn.*, 206:139–145, 1996.
- [24] Abu-Issa R., Waldo K., and Kirby M.L. Heart fields: one, two or more? *Developmental Biology*, 272(2):281–285, 2004.
- [25] Lyons I., Parsons L.M., Hartley L., Li R., Andrews J.E., Robb L., and Harvey R.P. Myogenic and morphogenetic defects in the heart tubes of murine embryos lacking the homeo box gene *nkx2-5*. *Genes & Development*, 9:1654–1666, 1995.
- [26] Ehrman L.A. and Yutzey K.E. Lack of regulation in the heart forming region of avian embryos. *Developmental Biology*, 207:163–175, 1999.
- [27] Jamali M., Rogerson P.J., Wilton S., and Skerjanc I.S. *Nkx2.5* activity is essential for cardiomyogenesis. *The Journal of Biological Chemistry*, 276(45):4225242258, 2001.

-
- [28] Charron F. and Nemer M. Gata transcription factors and cardiac development. *Cell and Developmental Biology*, 10:85–91, 1999.
- [29] Shirinsky V.P., Khapchaev A.Y., and Stepanove O.V. Molecular mechanisms of cardiomyogenesis and the prospects for cardiomyocyte regeneration in cardiac failure. *Molecular Biology*, 42(5):762772, 2008.
- [30] Morin S., Charron F., Robitaille L., and Nemer M. Gata-dependent recruitment of mef2 proteins to target promoters. *The EMBO Journal*, 19(9):2046–2055, 2000.
- [31] Christman J.K. 5-azacytidine and 5-aza-2'-deoxycytidine as inhibitors of dna methylation: mechanistic studies and their implications for cancer therapy. *Oncogenes*, 21:5483–5495, 2002.
- [32] Lee B.H., Yegnasubramanian S., Lin X., and Nelson W.G. Procainamide is a specific inhibitor of dna methyltransferase 1. *The Journal of Biological Chemistry*, 280(49):4074940756, 2005.
- [33] Broday L., Lee Y., and Costa M. 5-azacytidine induces transgene silencing by dna methylation in chinese hamster cells. *Molecular and Cellular Biology*, 19(4):31983204, 1999.
- [34] Antonitsis P., Papagiannaki E.I., Kaidoglou A., and Papakonstantinou C. In vitro cardiomyogenic differentiation of adult human bone marrow mesenchymal stem cells. the role of 5-azacytidine. *Biochemical and Biophysical Research Communication*, 341:320–325, 2006.
- [35] Xy W., Zhang X., Qian H., Zhu W., Sun X., Hu J., Zhou H., and Chen Y. Mesenchymal stem cells from adult human bone marrow differentiate into a cardiomyocyte phenotype in vitro. *Experimental Biology and Medicine*, 229:623–631, 2004.
- [36] Kadivar M., Khatami S., Mortazavi Y., Shokrgozar M.A., Taghikhani M., and Soleimani M. In vitro cardiomyogenic potential of human umbilical vein-derived mesenchymal stem cells. *Biochemical and Biophysical Research Communication*, 340:639–647, 2006.
- [37] Tomita S., Li R., Weisel R.D., Mickle D.A.G., Kim E., Sakai T., and Jia Z. Autologous transplantation of bone marrow cells improves damaged heart function. *Journal of the American Heart Association*, 100:247–257, 1999.
- [38] Fukuda K. Development of regenerative cardiomyocytes from mesenchymal stem cells for cardiovascular tissue engineering. *Artificial Organs*, 25(3):187–193, 2001.
- [39] Wu K.H., Mo X.H., Zhou B., Lu S.H., Yang S.G., Liu Y.L., and Han Z.C. Cardiac potential of stem cells from whole human umbilical cord tissue. *Journal of Cellular Biochemistry*, 2009.
- [40] Makino S., Fukuda K., Miyoshi S., Konishi F., Kodama H., Pan J., Sona M., Takahashi T., Hori S., Abe H., Hata J., Umezawa A., and Ogawa S. Cardiomyocytes can be generated from marrow stromal cells in vitro. *J. Clin. Invest.*, 103:697–705, 1999.

- [41] Wakitani S., Saito T., and Caplan A.I. Myogenic cells derived from rat bone marrow mesenchymal stem cells exposed to 5-azacytidine. *Muscle Nerve*, 18(12):1417–1426, 1995.
- [42] Liu Y., Song J., Liu W., Wan Y., Chen X., and Hu C. Growth and differentiation of rat bone marrow stromal cells: does 5-azacytidine trigger their cardiomyogenic differentiation? *Cardiovascular Research*, 58:460–468, 2003.
- [43] Yoo C.B., Cheng J.C., and Jones P.A. Zebularine: a new drug for epigenetic therapy. *Biochemical Society Transactions*, 32(6):910–912, 2004.
- [44] Lee W.J. and Kim H.J. Inhibition of dna methylation is involved in trans-differentiation of myoblasts into smooth muscle cells. *Molecules and Cells*, 24(3):441–444, 2007.
- [45] Li H., Yu B., Zhang Y., Pan Z., Xu W., and Li H. Jagged1 protein enhances the differentiation of mesenchymal stem cells into cardiomyocytes. *Biochemical and Biophysical Research Communication*, 341:320–325, 2006.
- [46] Planat-Bnard V., Menard C., Andr M., Puceat M., Perez A., Carcia-Verdugo J.M., Pnicaud L., and Casteilla L. Spontaneous cardiomyocyte differentiation from adipose tissue stroma cells. *Journal of American Heart Association*, 94:223–229, 2003.
- [47] Palpant N.J., Yasuda S., MacDougald O., and Metzger J.M. Non-canonical wnt signaling enhances differentiation of $sc\alpha^+$ / $c\text{-kit}^+$ adipose-derived murine stromal vascular cells into spontaneously beating cardiac myocytes. *Journal of Molecular and Cellular Cardiology*, 43:362–370, 2007.
- [48] Gaustad K.G., Boquest A.C., Anderson B.E., Gerdes A.M., and Collas P. Differentiation of human adipose tissue stem cells using extracts of rat cardiomyocytes. *Biochemical and Biophysical Research Communication*, 314:420–427, 2004.
- [49] Wang T., Xu Z., Jiang W., and Ma A. Cell-to-cell contact induces mesenchymal stem cell to differentiate into cardiomyocyte and smooth muscle cell. *International Journal of Cardiology*, 109:74–81, 2006.
- [50] Shim W.S.N., Jiang S., Wong P., Tan J., Chua L., Tan Y.S., Sin Y.K., Lim C.H., Chua T., Teh M., Liu T.C., and Sim E. Ex vivo differentiation of human adult bone marrow stem cells into cardiomyocyte-like cells. *Biochemical and Biophysical Research Communications*, 324:481–488, 2004.
- [51] Engler A., Bacakova L., Newman C., Hategan A., Griffin M., and Discher D. Substrate compliance versus ligand density in cell on gel responses. *Biophysical Journal*, 86:617–628, 2004.
- [52] Engler A., Griffin M.A., Sen S., Bnneman C.G., Sweeney H.L., and Discher D. Myotubes differentiate optimally on substrates with tissue-like stiffness: pathological implications for soft or stiff microenvironments. *The Journal of Cell Biology*, 166(6):877–887, 2004.
- [53] Deroanne C.F., Lapiere C.M., and Nusgens B.V. In vitro tubulogenesis of endothelial cells by relaxation of the coupling extracellular matrix-cytoskeleton. *Cardiovascular Research*, 49:647–658, 2001.

-
- [54] Wang Y. and Discher D.E. *Cell Mechanics*. Elsevier, 2007.
- [55] Kiernan J.A. Formaldehyde, formalin, paraformaldehyde and glutaraldehyde: What they are and what they do. *Microscopy Today*, 00(1):8–12, 2000.
- [56] Serway R.A. and Jewett J.W. *Physics for Scientists and Engineers, 6th Edition*. Thomson Brooks/Cole, 2004.
- [57] Boudou T., Ohayon J., Picart C., and Tracqui P. An extended relationship for the characterization of young's modulus and poisson's ratio of tunable polyacrylamide gels. *Biorheology*, 43:721–728, 2006.
- [58] Touhami A., Nysten B., and Dufrene Y.F. Nanoscale mapping of the elasticity of microbial cells by atomic force microscopy. *Langmuir*, 19(11):4539–4543, 2003.
- [59] Vinckier A. and Semenza G. Measuring elasticity of biological materials by atomic force microscopy. *FEBS Letters*, 430:12–16, 1998.
- [60] Mcpherson M.J. and Moller S.G. *PCR 2nd Edition*. Garland Publishing Inc, 2006.
- [61] Dorak T. *Real-time PCR*. Taylor & Francis Ltd, 2006.
- [62] Hunt M. *REAL-TIME PCR*, 2006. <http://pathmicro.med.sc.edu/pcr/realtime-home.htm>.
- [63] Bustin S.A. and Nolan T. Pitfalls of quantitative real-time reverse-transcription polymerase chain reaction. *Journal of Biomolecular Techniques*, 15:155–166, 2004.
- [64] Nolan T., Hands R.E., and Bustin S.A. Quantification of mrna using real-time rt-pcr. *Nature Protocols*, 1(3):1559–1582, 2006.
- [65] Pelham R.J. and Wang Y. High resolution detection of mechanical forces exerted by locomoting fibroblasts on the substrate. *Molecular Biology of the Cell*, 10:935–945, 1999.
- [66] Breuls R.G.M., Klumpers D.D., Everts V., and Smit T.H. Collagen type v modulates fibroblast behavior dependent on substrate stiffness. *Biochemical and Biophysical Research Communications*, 380(2):425–429, 2009.
- [67] Flanagan L.A., Ju Y., Marg B., Osterfield M., and Janmey P.A. Neurite branching on deformable substrates. *NeuroReport*, 13(18):2411–2415, 2002.
- [68] Li L., Sharma N., Chippada U., Jiang X., Schloss R., Yarmush M.L., and Langrana N.A. Functional modulation of es-derived hepatocyte lineage cells via substrate compliance alteration. *Annals of Biomedical Engineering*, 36(5):865–876, 2008.
- [69] Pierce Protein Research Products. *Sulfo-SANPAH Photoreactive Crosslinker*, 2009. <http://www.piercenet.com/Objects/View.cfm?type=ProductFamily&ID=02030372&Format=Print>.

- [70] Ideno A., Yoshida T., Iida T., Furutani M., and Maruyama T. Fk506-binding protein of the hyperthermophilic archaeum, thermococcus sp. ks-1, a cold-shock-inducible peptidyl-prolyl cistrans isomerase with activities to trap and refold denatured proteins. *Biochem. J.*, 357:465–471, 2001.
- [71] Wang H.B., Dembo M., and Wang Y.L. Substrate flexibility regulates growth and apoptosis of normal but not transformed cells. *Am. J. Physiol.*, 279:13451350, 2000.
- [72] Hofman S., Knecht S., Langer R., Kaplan D.L., Vunjak-Novakovic G., Merkle H.P., and Meinel L. Cartilage-like tissue engineering using silk scaffolds and mesenchymal stem cells. *Tissue Engineering*, 12(10):2729–2738, 2006.
- [73] Markoullis K., Bulian D., Hlzlwimmer G., Quintanilla-Martinez L., Heiliger K.J., Zitzelsberger H., Scherb H., Mysliwicz J., Uphoff C.C., Drexler H.G., Adler T., Busch D.H., Schmidt J., and Mahabir E. Mycoplasma contamination of murine embryonic stem cells affects cell parameters, germline transmission and chimeric progeny. *Transgenic Research*, 18(1):71–87, 2009.
- [74] Garner C.M., Hubbard L.M., and Chakraborti P.R. Mycoplasma detection in cell cultures: a comparison of four methods. *British Journal of Biomedical Science*, 57(4):295–301, 2000.
- [75] Olson L.D. and Barile M.F. Mycoplasma infection of cell cultures: Isolation and detection. *Journal of Tissue Culture Methods*, 11(3):175–179, 1988.
- [76] *Personal conversation with Trine Fink.*
- [77] Samani A., Bishop J., Luginbuhl C., and Plewes D.B. Measuring the elastic modulus of ex vivo small tissue samples. *Phys. Med. Biol.*, 48:2183–2198, 2003.
- [78] Samani A., Zubovits J., and Plewes D. Elastic moduli of normal and pathological human breast tissues: an inversion-technique-based investigation of 169 samples. *Phys. Med. Biol.*, 52:1565–1576, 2007.
- [79] Tontonoz P., Hu E., Devine J., Beale E.G., and Spiegelman B.M. Ppar γ 2 regulates adipose expression of the phosphoenolpyruvate carboxykinase gene. *Molecular and Cellular Biology*, 15(1):351–357, 1995.
- [80] Tontonoz P., Hu E., and Spiegelman B.M. Regulation of adipocyte gene expression and differentiation by peroxisome proliferator activated receptor γ . *Current Opinion in Genetics and Development*, 5(5):571–576, 1995.
- [81] Lee W.C., Sepulveda J.L., Rubin J.P., and Marra K.G. Cardiomyogenic differentiation potential of human adipose precursor cells. *International Journal of Cardiology*, 2008.
- [82] Safford K.M., Hicok K.C. Safford S.D., Halvorsen Y.C., Wilkison W.O., Gimble J.M., and Rice H.E. Neurogenic differentiation of murine and human adipose-derived stromal cells. *Biochemical and Biophysical Research Communications*, 294:371–379, 2002.

- [83] Anghileri E., Marconi S., Pignatelli A., Cifelli P., Gali M., Sbarbati A., Krampera M., Belluzzi O., and Bonetti B. Neuronal differentiation potential of human adipose-derived mesenchymal stem cells. *Stem Cells and Development*, 17:909–916, 2008.
- [84] Bartunek J., Croissant J.D., Wijns W., Gofflot S., de Lavareille A., Vanderheyden M., Kaluzhny Y., Mazouz N., Willemsen P., Penicka M., Mathieu M., Homsy C., De Bruyne B., McEntee K., Lee I.W., and Heyndrickx G.R. Pretreatment of adult bone marrow mesenchymal stem cells with cardiomyogenic growth factors and repair of the chronically infarcted myocardium. *Am J Physiol Heart Circ Physiol*, 292(2):1095–1104, 2007.
- [85] Kawai T., Takahashi T., Esaki M., Ushikoshi H., Nagano S., Fujiwara H., and Kosai K. Efficient cardiomyogenic differentiation of embryonic stem cell by fibroblast growth factor 2 and bone morphogenetic protein 2. *Circ J*, 68:691–702, 2004.
- [86] Li Z., Dranoff J.A., Chan E.P., Uemura M., Svigny J., and Wells R.G. Transforming growth factor- β and substrate stiffness regulate portal fibroblast activation in culture. *Hepatology*, 46:1246–1256, 2007.
- [87] Tomasek J.J., Gabbiani G., Hinz B., Chaponnier C., and Brown R.A. Myofibroblasts and mechanoregulation of connective tissue remodelling. *Nature Reviews*, 3:349–363, 2002.

Appendix A

Chemicals and Equipment

A.1 Chemicals

- 2-mercaptoethanol (Sigma, lot:119H091415)
- 2-(N-morpholino)ethanesulfonic acid (MES)
- 4-(2-hydroxyethyl)-1-piperazineethanesulfonic acid (HEPES) (Sigma, lot: 110H5606)
- 5-azacytidine (Sigma, lot: 085K1650)
- Acetic acid (Merck, lot: K38324563 803)
- Acrylamide 40% (Bie & Berntsen, lot: 27060)
- Acrylic acid (Aldrich, lot: 571334-089)
- Alexa fluor 555 antimouse IgG (Invitrogen, lot: 49958A)
- Ammonium persulphate (APS) (Sigma, lot: 104K0456)
- Bind-silane (Pharmacia Biotech, lot: 431K20705789)
- Bovine Serum Albumin, BSA (Europe Bioproducts, BAH62-673)
- Collagen type I from rat tail (Sigma, lot: 058K3808)
- DNase I (Sigma, lot: 066K6091)
- DNase digest buffer (Sigma, 027K6069)
- Ethanol 96% (Kemetyl, lot: 0607026362)
- Ethylene Diamine Tetraacetic Acid, EDTA (VWR, lot: K15729118)
- Fetal Bovine Serum, FBS (VWR, lot: 40Q6242F)
- Fibronectin 0.1% from bovine plasma (Sigma, lot: 116K7560)
- Formaldehyde 3.7% (VWR, lot: 040907-005)
- Gentamicin (VWR, lot: 14434)
- Hydrogen peroxide (H₂O₂) 30% (Merck, lot: K11609409)
- Insulin solution from bovine pancreas (Sigma, lot: 11K8416)
- Ischoves MDM (Gibco, lot: 463864)
- Iscript 5x reaction mix (Biorad, lot: 4206447)
- Iscript reverse transcriptase (Biorad, lot: 4206445)
- L-glutamine (VWR, lot: 441387)
- MEM alpha medium + Glutamax (Gibco, lot: 360212)
- Methocult M3134 (StemCell Technologies, cat: 03134)
- Monoclonal anti collagen type 1 clone COL-1 (Sigma, lot: 81K4897)
- Monoclonal anti fibronectin, produced in mouse (Sigma, lot: 077K4853)
- N-ethyl-N-(3-dimethylaminopropyl)carbodiimide hydrochloride (Sigma, lot: 076K0668)
- N-hydroxysuccinimide (Fluka, lot: 1184854)
- N,N-methylene-bis-acrylamide (Sigma, lot: 077K1802)
- N,N,N,N-tetramethylethylenediamine (TEMED) (ICN Biomedicals, lot: 18334)
- Natrium hydroxide (Bie & Berntsen, lot: 518737)
- Nuclease free water (Biorad, lot: 4206448)
- OPD (ortho-phenyldiamin) tablets (DAKO, lot: S2045)
- Recombinant human interleukin-3 (R&D Systems, cat: 203-IL)
- Recombinant human Interleukin-6 (R&D Systems, cat: 206-IL)
- Recombinant human stem cell factor (R&D Systems, cat: 255-SC)
- Repel-silane (Pharmacia Biotech, lot: A6-1032)

- Ribonuclease inhibitor from human placenta (Sigma, lot: 058K37900)
- Penicillin + Streptomycin (VWR, lot: 1363577)
- Secondary antibody rabbit polyclonal anti-mouse immunoglobulin horseradish peroxidase labeled (DAKO, lot: P0260)
- Sterilized phosphate buffered saline, S-PBS
- Sulfosuccinimidyl-6-(4'-azido-2'-nitrophenylamine) hexanoate (sulfo-SANPAH) (Soltec Ventures, lot: SV041214)
- Sulfuric acid (H₂SO₄) (Bie & Berntsen, lot: LAB00531)
- SYBR green supermix (Biorad, lot: 10003253)
- Total RNA elution solution (Biorad, lot: C9704332)
- Total RNA high stringency buffer (Biorad, lot: C9704328)
- Total RNA human adult skeletal muscle (Capital Biosciences, lot: B207204)
- Total RNA low stringency buffer (Biorad, lot: L9704330)
- Total RNA lysis solution (Biorad, lot: L9704326)
- Transferrin (Roche, cat: 11966400)
- Triton X-100 (Sigma, lot: 122H0766)
- Trypan Blue 0.4% (Sigma, Cat. no: T-8154)
- Trypsin (VWR, lot: 71704)
- Tween20 (Acros organics, lot: A0235351)
- Zebularine (Sigma, lot: 037K46153)

A.2 Equipment

- Atomic Force Microscope (Veeco Nanoscope IIIA, sn: 2080EX)
- Axiovert 200M (Zeiss, sn: 034-007314)
- Axio Observer.z1 (Zeiss, sn: 3834000216)
- Biorad Icyler Thermal Cycle (Biorad, sn: 582BR 016089)
- Centrifuge tube 15 ml (Greiner-bioone cat: 430791)
- Centrifuge tube 50 ml (Greiner-bioone cat: 227261)
- GeneAmp PCR system 2400 (Perkin Elmer, sn: 80337071126)
- Hemocytometer
- Nanodrop ND-1000 (Saveen Werner, sn: 3211)
- Needle 1 ml (Once, lot: A89189-1)
- Non-conductive silicon nitride cantilever (Veeco, cat: NP-20)
- Olympus CKX41 (Olympus, sn: 5B16020)
- PCR plates
- PST 6-well container (Corning Inc. cat: 3506)
- PST 12-well container (Corning Inc. cat: 3512)
- PST 24-well container (Corning Inc. cat: 3524)
- PST 48-well container (Corning Inc. cat: 3548)
- PST 96-well container (Corning Inc. cat: 3596)
- PST flasks (Greiner-bioone cat: 658-175)
- UV Stratalinker 1800 (Stratagene, sn: 000193112167)
- VICTOR² 1420 Multilabel Counter (Wallac, sn: 4200682)

Appendix B

Culturing: Areas and Volumes

Culturing area	S-PBS	T+E	Medium
25 cm ² Bottle (T25)	5 ml	1 ml	6 ml
75 cm ² Bottle (T75)	10 ml	1.5 ml	15 ml
175 cm ² Bottle (T175)	14 ml	3 ml	30 ml
0.32 cm ² 96-Well plate (per well)	0.3 ml	0.1 ml	0.2 ml
0.80 cm ² 48-Well plate (per well)	0.3 ml	0.1 ml	0.3 ml
1.9 cm ² 24-Well plate (per well)	0.5 ml	0.3 ml	1 ml
3.8 cm ² 12-Well plate (per well)	0.5 ml	0.3 ml	1.5 ml
9.2 cm ² 6-Well plate (per well)	1 ml	1 ml	4 ml
0.8 cm ² 8-Well slide (per well)	0.3 ml	0.1 ml	0.3 ml
1.8 cm ² 4-Well slide (per well)	0.5 ml	0.3 ml	0.5 ml
4.2 cm ² 2-Well slide (per well)	0.5 ml	0.3 ml	1 ml
9.4 cm ² 1-Well slide (per well)	1 ml	0.5 ml	2 ml
78 cm ² 100 mm petri dish	10 ml	3 ml	15 ml

Table B.1: *The appropriate S-PBS, T+E and medium volumes in regard to culturing area.*

Appendix C

Primers

Primers used for investigating the differentiation of ASCs. Before use the primers were diluted to a concentration of $10 \mu M$ and they were optimized in order to determine the annealing temperature and to make sure that the primers did not form any primer-dimer complexes.

Gene description	Symbol	Target	Primer sequence (5'-3')
GATA binding protein 4	GATA-4	Cardiac muscle	f-GCC TGG CCT GTC ATC TCA CT r-ACA TCG CAC TGA CTG AGA ACG f-CCC TGC CTT CTA CTC AAA GC r-CGT GTG TTG TGG GTA TCT CG
Myocyte enhancer factor 2C	MEF2C		f-CAG GAT GGC AAA GAC TAC ATT G r-GAG GAT TCT GGA CTC TCT CTG CC f-OGG CTT GCA CCAAT CAG C r-GAT GAG AGC CTC CAG GAT GG
Vascular endothelial growth factor 2	VEGFR-2	Endothelium	f-AAA GGA CGA GTT CTA TGA CG r-AGT GCT CTT CGG GTT TCA GG f-TGA TTG AGG GTA GGT TGT TGC r-CAC CAG AGA CAT TTT GAT GAG C
Von Willebrand factor	VWF		f-TAA GGT GAA AAG GGG TGT GG r-CCT ACA GCC TCG ATT CTT GG f-CCC TGT CTA TTG CTC CAT CC r-CCT TGC TTG TTC TGC TTG C
Myogenic differentiation 1	MYOD1	Skeletal muscle	f-CAC ACA GCT CAC TCG ACC TTG r-TTC GGT TAT TTT TAG GAT CAT CTC G f-GGC AAT AGC AGG TTC ACG TAC A r-CGA TAA CAG TCT TGC CCC ACT T
Myogenic Factor 5	MYF5		f-GGC CTG GAT CTT CTT TCT CC r-CCT CTG CCA CAG TTT CCT TC f-GGC AGC ACG CTA TTA AAT CC r-GTC GCC AAA CAG ATT CAT CC
Nestin	NES	Nervous tissue	f-CCA CAG GCC GAG AAG GAG AAG C r-GCC AGG GCC CGG AGG AGG TCA G f-ATG GGA TGG AAA ATC AAG CA r-GTG GAA GTG ACG CCT TTC AT
Neuronal growth factor receptor, p75	NGFR		f-ACT TTT GGT SCS TTG TGG CTT CAA r-CCG CCA GGA CAA ACC AGT AT f-GAA TCT CCC CTC CTC ACA GTT G r-GGC CCC TCC CCT CTT CA
Sex Det. Region Y-box 9	SOX9	Cartilage	f-TCC TGG CAT CTT GTC CAT G r-CCA TCC AAC CAC TCA GTC TTG
Collagen II Alpha 1	COL2A1		
Osteonectin	ONN	Bone tissue	
Runt-related transcription factor 2	RUNX2		
Peroxisome prolifer.-activa. Reprtr. gam. 2	PPAR γ 2	Adipose tissue	
Fatty acid binding protein 4	AP2		
Tyrosine 3-monooxygenase/tryptophan 5-monooxygenase activation protein, zeta polypeptide	YWHAZ		
Glyceraldehyde 3-phosphate dehydrogenase 3	GAPDH-3	Housekeeping	
Cyclophilin A	PPIA		

Appendix D

Methylcellulose-based Medium

Total yield: 2ml

- 800 μ l Methocult M3134
- 847 μ l Ischoves MDM
- 300 μ l FCS
- 0.02 g BSA
- 20 μ l L-glutamine
- 13.3 μ l transferrin
- 2 μ l insulin
- 2 μ l IL-3
- 2 μ l IL-3
- 10 μ l SCF
- 4 μ l 2-mercaptoethanol

All ingredients, except Methocult M3134, were mixed before adding ACS to the medium.
After the addition of ASCs, Methocult M3134 was added.